university of groningen / faculty of mathematics and natural sciences

Revision on Vacuum Entropy Numerics

and the Black Hole Information Problem

Ernst D. Stam
SUPERVISOR: Kyriakos Papadodimas

ABSTRACT

By means of a revision of the articles by Mark Srednicki and John Cardy some results are presented on free scalar field vacuum entanglement entropy numerics. In particular, an attempt was made to use and expand numerical methods from Srednicki's paper to confirm a law on the mutual information of two spheres at large distances. The expansion of methods include generalisation to any discrete concentric set regions. To leading order the area law for shell-like regions was confirmed. Numerical results on Renyi entropies, defined by the Renyi parameter q, are presented and area law coefficients $\alpha(q)$ are compared. Some context is provided by a quick review of the black hole information problem.

Contents

I

Introduction

Coarsely this thesis consists of three parts. The first part scratches the surface of the black hole information paradox and problem. The surface of some work of Hawking [1], Susskind et Thorlacius [2] and Mathur [3] is scratched to create an urge for investigation of the topic treated in this thesis. The black hole information paradox, which still occupies many physicists today, motivates a thorough research into entanglement entropy. All the more since, to the authors opinion, the position of for example Mathur on the black hole information paradox, [4, 5], is based on an incomplete quantitative knowledge of vacuum entropy and information. The last section of this chapter treats this motivation in more detail.

The above-mentioned automatically leads to the second part that narrows the scope to particular, highly symmetric computations of vacuum entanglement entropy. Here, a review is given of two important articles by Srednicki [6] and Cardy [7] which discuss methods to actually calculate the vacuum entanglement entropy and mutual information of certain specific regions in a free field theory.

The third part attempts a possible connection between the previously mentioned articles. It largely consists of numerical computation, but only with the intention to verify the analytical results reviewed in the previous part. Due to a conformal mapping a slightly extended version of the calculations by Srednicki can be compared with the mutual information law of two distant spheres described by Cardy. Targeting this comparison, some other results, that arose from the computational framework in use, are treated and compared to foregoing articles [8, 9].

The text is aimed to be as complete and self containing as possible for a reader with some experience in general relativity and quantum field theory. Sections I.1 and II.1 were added to provide a subject specific basis in the fields of the black hole information problem and quantum information theory. For further reading on the the black hole information problem see [10–12]. Some articles on entanglement entropy are [13–18].

I.1. Black Hole Paradox and Problem

"All war is symptom of a man's failure as a thinking animal.", written by Steinbeck [19], could be used to refer to the scientific 'Black Hole War' fought between Hawking and Thorne on one side and Preskill, Susskind and 't Hooft on the other side. It could hint that we have to reinvent ourselves as thinking animals. Or do we need something less feral, a machine perhaps? Srednicki showed that numerics could, with the uv-cutoff being the sole approximation, check the area law from Susskind's gedanken experiment mentioned below.

First note that there is a difference between the black hole information paradox and the black hole problem.

The black hole paradox arises from the fact that, to ensure the smoothness of the horizon, Hawking pairs, one falling in and the other escaping towards infinity being responsible for the return of information, should be (maximally) entangled to each other. However, to ensure unitarity of the S-matrix, the second particle should also be entangled with all previously emitted Hawking radiation. This is not allowed by the principle of monogamy of quantum entanglement. Although the black hole information paradox seems challenging enough, some very reasonable arguments, discussed again in section V.3, have been presented, [2,20], that seem to debunk it.

The black hole information problem is about finding a consistent description of the creation and evaporation of a black hole, including a mechanism that connects the infra-red and ultraviolet worlds. It is the real hard problem.

I.2. A brief History of the Black Hole

Susskind [21] poetically describes how gedanken experiments involving paradoxes can shift paradigms. There are four fundamental physical principles which are in conflict with each other. When doing quantum field theory in the vicinity of a black hole horizon it was shown that unitarity, the equivalence principle, the quantum Xerox principle and locality can not all be obeyed at the same time.

When Hawking first discovered his radiation [1, 22, 23] and together with Bekenstein the entropy law for Black Holes [24], he was under the impression that in a fine grained sense information would be lost in the process of Black Hole creation and evaporation. He reasoned that, if one of two particles forming a correlated pair falls in, the density matrix would not be pure after evaporation, or the information would be restored when the black hole is 'exposed' at the end of the process. However, Susskind reasoned that the maximum of information stored in a region is its entropy and thus the black hole must start emitting information once it has evaporated past half its original value.

A second proposal is the black hole complementarity concept by Susskind et al. [21, 25], which in some sense violates locality. It states that there is no contradiction for any observer. An external observer will see that a black hole can store information up to a maximum, that is its entropy. Information can be absorbed, thermalised and re-emitted and the fine grained entropy is always less than the black hole entropy. The freely infalling observer can not distinguish between acceleration and curvature and for a large enough black hole it experiences

nothing out of the ordinary. A possible contradiction could occur if the infalling observer receives information about himself through reflected Hawking radiation, or if a second observer hoovering near the horizon decides to jump in with the received Hakwing bits. The quantum xerox principle appears to be violated which could be a problem for the complementarity principle. However, it is important to realize that it is impossible in quantum mechanics to send arbitrary amounts of information in a certain short amount of time with a limited amount of energy. The quantum Xerox principle is maintained due to the inequality $E_{\text{info}} \gg M_{\text{BH}}$, [26–28].

Another possibility is violating the equivalence principle. In a paper by Almheiri, Marolf, Polchinski and Sully, [4], the so called firewall is proposed. With use of the strong sub-additivity of entropy, it is argued that entanglement at the (stretched) horizon has to be broken creating an intense wall of high energy quantum modes near the horizon. A somewhat similar proposal by Mathur et al. [3, 5, 29] describes a stringy fuzzball with the same radius as a classical Schwarzschild black hole. In his paper, which does away with the no-hair theorem, he argues that small corrections on 'smooth' space like slices can never turn the entropy around after the Page time. It is clear that these theories disqualify classical relativity as a description of universes containing black holes. This is a bit counter intuitive since it was general relativity which predicted the existence of the Schwarzschild solution altogether.

Furthermore, some interesting perspectives are provided form the Ads/CFT community by Papadodimas and Raju, [30]. Lastly semi-unitary qubit models from information theory by Avery [31] should be mentioned.

I.3. Motivation

From the brief historical introduction of the black hole paradox above it is clear that qualitative notions from gedanken experiments alone might be enough to describe it, but call for thorough quantitative models describing the streams of information around the horizon. It is important to realize that more precise yet perhaps more creative ways of describing information are needed to answer questions risen by fantastic proposals to resolve the paradox. There is, for example, still disagreement on the disability of small corrections on the 'near' thermal density matrix to turn the Page curve around. How does the thermal nearness relate to the vastness of the Hilbert space?

It is worth noting that, to resolve the black hole information paradox or unitarise the S-matrix, non-locality needs to be violated only in the order of $\exp(-\dim \mathscr{H}_{BH})$. For a solar mass black hole this means that the non-local entanglement between two states (or Hawking particles) should be of the order $e^{-10^{77}}$.

One can at least say that perturbative non-local effects should be able to turn the Page curve around and allow for a S-matrix description of black hole creation and evaporation. However, how to make such a process precise is still a mystery and therefore all sorts of detailed and quantitative research on (vacuum) entanglement are of particular interest.

Moreover, it is in general still a challenge to accurately and universally define entanglement entropy. In QFT's, the usual framework of vacuum quantum mechanics, entanglement entropy is divergent. Any quantitative measure of entanglement entropy therefore depends

on the regularisation method and uv-cutoff. The methods of Cardy described below, giving the mutual information in a special case with free fields, are precise and therefore rare and of special interest.

All in all it seems wise to further explore the path set in by Srednicki and build a numerical framework to be able to check claims done in the field. As will be explained in the coming text, the goal is to check a formula derived by Cardy using a method build on the foundation laid by Srednicki. Of course many other ideas could be checked with similar methods, however the small time scales we live our life in prevented execution of them. Some more comments on possible future extensions can be found in the discussion, section V.2.

II

Theory

In this analytical chapter entanglement entropy is treated in general first. The quantum mechanical counterparts of the Shannon and Renyi entropies lie at the basis of most numerical approaches regarding entanglement. In the case of QFT over sub-regions of space, it is possible to assign Hilbert sub-spaces to these sub-regions and thereby construct a density matrix which allows for entropy computation. Secondly, before reviewing the derivation of the mutual information, it is convenient to put a bit more emphasis on the so called replica trick, as Cardy puts it in [7]. Therefore [32] and [33] are revisited shortly to make this chapter as self containing as possible. Thirdly, the Renyi mutual information and ultimately the mutual information for two disjoint spheres are derived. This chapter then ends with Srednicki's famous area law for the von Neumann entropy ($q = 1$) in a brief review of [6]. In general the area law is

$$S(A, \bar{A}) = \frac{\alpha(q)}{\nu^2} R^2, \tag{II.0.1}$$

with R the radius of spherical region A, q the Renyi-parameter and ν the uv-cutoff. The last section forms a bridge to the numerical methods used to calculate the inverse shell mutual information, which are described in the next chapter.

II.1. On Entanglement Entropy

To investigate quantum entanglement in general the entanglement entropy is used as a measure of it. Entropy originated in three separate places. Firstly it came up in the search of lost energies in heat engines and was proposed by Claussius as an important thermodynamic quantity. Secondly Boltzmann formulated entropy as statistical 'mixedupness' of a system. In 1948 Shannon [34], who investigated information processes, derived the measure of information $S(p_1, \ldots, p_n)$ we now call entropy from 3 simple requirements. Let $\{p_1, \ldots, p_n\}$ be a set of probabilities of n possible events in a system, then

- S should be continuous in the p_i;

- if all p_i are equal, that is $p_i = 1/n$, then S should be a monotonically increasing function of n;
- if a choice is broken down in two choices, imagine throwing 2 dice separately instead of simultaneously, S_{tot} is the weighted sum of the individual values of S_j.

It resulted in the formula

$$S = -K \sum_{i=1}^{n} p_i \ln p_i .$$

He found out that his formulation of information had the same structure as the statistical or thermodynamical entropy and got the hint from von Neumann to call it as such.

It is important to realise that a quantum field theory and its vacuum can be viewed as an ensemble. Moreover, a statistical mixture of one spacial region with the rest of space can be elegantly expressed through the density matrix which has a dimension equal to the dimension of the Hilbert space describing the system.

Suppose a quantum system is in a pure state $|\Psi\rangle$, and has density matrix $\rho = |\Psi\rangle\langle\Psi|$, and only a subset A, belonging to region A with $\mathscr{H}_A$ the Hilbert sub-space, of a complete set, that is $A + \overline{A}$, of commuting observables is measured. The reduced density matrix is $\rho_A = \text{Tr}_{\bar{A}}(\rho)$ and the entanglement entropy is the von Neumann entropy

$$S_A = -\text{Tr}\,\rho_A \log \rho_A \,. \tag{II.1.1}$$

It is the quantum mechanical counter part of the Shannon entropy $H_1(X) = -\sum_{i=1}^{m} p_i \log p_i^n$, which again is obtained by taking he limit $n \to 1$ of the Renyi Entropy.

$$H_n(X) = \frac{1}{1-n} \log\left(\sum_{i=1}^{m} p_i^n\right) \qquad \text{(information theory)} \tag{II.1.2a}$$

$$S_A^{(n)} = \frac{1}{1-n} \log\left(\text{Tr}\,\rho_A^n\right) \qquad \text{(quantum mechanics)} \tag{II.1.2b}$$

Some properties of the entanglement entropy are that $S_A = S_{\bar{A}}$, which is easy to see since A and $\bar{A}$ can only be entangled to each other if they form a pure state; $S_A = 0$ for an unentangled product state and S_A is a maximum for a maximally entangled state.

There also exists a measure for correlation between to (non-complementary) subsystems called mutual information. In information theory it describes the random variables on which two subsystems are mutually dependent. The mutual information $I(A,B)$ of two disjoint regions is also calculated as the limit $n \to 1$ of the Renyi mutual information given by

$$I^{(n)}(A,B) = S_A^{(n)} + S_B^{(n)} - S_{A\cup B}^{(n)} \,. \tag{II.1.3}$$

As mentioned before, in general it is hard to evaluate the entanglement entropy of a subregion for an arbitrary QFT for all other spaces than $1+1$-dimensional ones, see [35]. However, Cardy found some techniques to do it in certain symmetrical cases, as will become clear in the next two sections.

II.2. The Replica Trick in 1 + 1 Space-time

This section provides a hand-waving summary of the basic principles used by Cardy, Tonni and Calabrese in [7, 33] which are called the replica trick. In one sentence it summarises to: calculate the Renyi entanglement entropy $S^{(n)}$ by performing an Euclidean path integral on a n-sheeted conifold, a manifold with certain topology which will become clear further on, where one lets $n \to 1$ for the von Neumann entropy.

Consider a quantum field theory with 'uv-cutoff' ν on the infinite line at $\tau = 0$ on a 2 dimensional manifold. Here τ is the imaginary time due to a rotation to Euclidean space-time. The cutoff functions as a lattice spacing and the sites are labelled by x. A complete set of observables $\{\hat{\phi}_x\}$ has the eigenstates $\{\phi_x\}$. Imagine a slice at $\tau = 0$ with a region A with a Hilbert space $\mathscr{H} = \mathscr{H}_A \times \mathscr{H}_{\bar{A}}$. The density matrix $\rho_{ij} = \langle i \,|\, \hat{\rho} \,|\, j \rangle$ in a state of a region A can be written as a path integral over imaginary Euclidean time. The fields over which the integration runs just above and below the slice in region A play the role of the i, j basis.

$$\rho\left(\{\phi_x\}, \{\phi'_{x'}\}\right) = Z^{-1} \int [d\phi(y,\tau)] \prod_x \delta(\phi(y,0^-) - \phi_x) \prod_x \delta(\phi(y,0^+) - \phi'_{x'}) e^{-S_E} \tag{II.2.1}$$

The effect of this integral is that the edges along $\tau = 0^-$ and $\tau = 0^+$ are sewed together. To ensure $\operatorname{Tr}\rho = 1$ one can set $\{\phi_x\} = \{\phi'_{x'}\}$ and integrate to obtain the proper normalization factor. Since the Euclidean action S_E does not depend explicitly on the Riemann surface the cylinder can be replaced by a cyclic manifold where along the line $\tau = 0$ segments can be sewed together. Given a region (or subset) $\{\phi_x\}_A$, the reduced density matrix ρ_A is found by applying this sewing procedure only to the complementary subset $\{\phi_x\}_{\bar{A}}$ and leaving sections cut out along the line $\tau = 0$ in the manifold. Now consider n of these manifolds, labelled by an integer j, containing N sections, labelled k, cut out at $\tau = 0$. For all $x \in A$ these n copies are sewed together cyclically in such a way that

$$\phi_j(x,0^+) = \phi_{j+1}(x,0^-) \qquad \text{and} \qquad \phi_n(x,0^+) = \phi_1(x,0^-).$$

This defines a n-sheeted Riemann surface with genus $(n-1)(N-1)$, called a conifold, on which a path integral can be done to compute $\operatorname{Tr}\rho_A^n$. Adopting the notation of Calabrese and Cardy, the path integral can be written as $Z_n(A)$ giving

$$\operatorname{Tr}\rho_A^n = \frac{Z_n(A)}{Z^n}. \tag{II.2.2}$$

The left hand side of this equation can be written as $\operatorname{Tr}\rho_A^n = \sum_\lambda \lambda^n$, where λ are the eigenvalues of the density matrix. Due to the normalization and the fact that all eigenvalues lie in the interval $[0,1)$, the left hand side is absolutely convergent and analytic for all real $n > 1$. This enables differentiation with respect to n in this domain.

II.3. Review of Cardy's 2013 Paper

In [7] the replica trick was applied using a free scalar field on a higher dimensional space to compute the mutual information of two spheres of sizes $R_{A,B}$ at a distance r. The result is

$$I(A,B) \sim \frac{4}{15}\left(\frac{r_i r_o}{r^2}\right)^2.$$

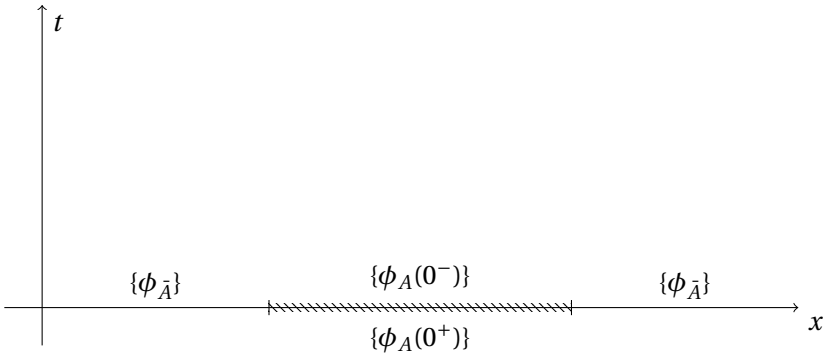

Figure 1: Schematic picture of one Riemann sheet containing one cut out section.

This result is of interest due to the conformal mapping which enables comparison with the numerical results given in IV.3. Some parts of this article therefore are reviewed in order to make this text more self containing. Section 2 is reviewed shortly to elaborate the general principle behind the expansion for $R_{A,B} \ll r$ Then section 3.2 and in particular section 3.2.1 are revisited to reveal the origin of the result above and its conformal translation to spherically symmetric spaces, that are adequate for numerics, in eqs. (II.4.5) and (II.4.6).

II.3.1. General from of the expansion for $R_{A,B} \ll r$.

Let a $d+1$ dimensional quantum field theory in $\mathbb{R}^d$ be in its ground state $|0\rangle$. Given a uv-cutoff and a decomposable Hilbert space, the Renyi entropies are given by eq. (II.1.2b). By the same principle as discussed in section II.2 the ground state wave functional, $\langle\{\psi\}|0\rangle_-$ or $\langle 0|\{\psi\}\rangle_+$, is given by an imaginary time path integral over the half space $\mathbb{H}_\pm$, which covers the space time between $\tau = \pm\infty$ and $\tau = 0$. Imagine n copies of the half spaces which are sewn together along $\tau = 0$ like in the $1+1$ example. This creates a conifold $C_A^{(n)}$ with a $d-1$-dimensional sub-manifold of conical singularities along the boundary $\partial A \cap \tau = 0$ and gives an expression for the trace of the reduced density matrix.

$$\mathrm{Tr}\,\rho_A^{(n)} = \frac{Z(C_A^{(n)})}{Z^n}$$

Let A and B be two disjoint regions, then the Renyi mutual information from eq. (II.1.3) can be written as

$$I^{(n)}(A,B) = \frac{1}{n-1}\log\left(\frac{Z(C_{A\cup B}^{(n)})Z^n}{Z(C_A^{(n)})Z(C_B^{(n)})}\right). \tag{II.3.1}$$

The term $Z(C_{A\cup B}^{(n)})$ is only computable for 1 space dimension, up to now. However, for $R_A, R_B \ll r$ an expansion is possible in terms of $R_A R_B / r^2$, see [33]. This expansion is the effect of locality and the operator product expansion in a CFT, similar to the cluster decomposition principle in a normal QFT. An observer far from regions A or B will not notice the conifold he is living on. To him, the seam seems a weighted sum of products of local operators $\Phi_{k_j}^{(j)}$ at a point

(r_A, r_B) inside each of the regions, where j numbers the copies of $\mathbb{R}^{d+1}$, written

$$\frac{Z(C^{(n)}_{A\cup B})}{Z^n} = \left\langle \Sigma^{(n)}_A \Sigma^{(n)}_B \right\rangle_{(\mathbb{R}^{(d+1)})^n} \tag{II.3.2}$$

where

$$\Sigma^{(n)}_A = \frac{Z(C^{(n)}_A)}{Z^n} \sum_{\{k_j\}} c^A_{\{k_j\}} \prod_j^{n-1} \Phi_{k_j}(r^{(j)}_A). \tag{II.3.3}$$

The k_j label the complete set of operators on the jth copy. Now consider $C^{(n)}_A$ and an arbitrary set of local operators away from A. Note that for a CFT the local operators can be chosen in such a way that $\langle \Phi_{k'}(r_X)\Phi_k(r_A)\rangle = \delta_{k'k}/|r_X - r_A|^{2x_k}$ for all separations, with x_k the scaling dimension.

$$\begin{aligned}
\left\langle \prod_{j'} \Phi_{k'_{j'}}(r^{(j')}_X) \right\rangle_{C^{(n)}_A} &= \left\langle \left(\prod_{j'} \Phi_{k'_{j'}}(r^{(j')}_X) \right) \left(\sum_{\{k_j\}} c^A_{\{k_j\}} \prod_{j=0}^{n-1} \Phi_{k_j}(r^{(j)}_A) \right) \right\rangle_{(\mathbb{R}^{d+1})^n} \\
&= \sum_{\{k_j\}} c^A_{\{k_j\}} \left\langle \left(\prod_{j'} \Phi_{k'_{j'}}(r^{(j')}_X) \right) \left(\prod_{j=0}^{n-1} \Phi_{k_j}(r^{(j)}_A) \right) \right\rangle_{(\mathbb{R}^{d+1})^n} \\
&= \sum_{\{k_j\}} c^A_{\{k_j\}} \prod_j \left\langle \Phi_{k'_j}(r^{(j)}_X)\Phi_{k_j}(r^{(j)}_A) \right\rangle_{(\mathbb{R}^{d+1})^n} \\
&= \sum_{\{k_j\}} c^A_{\{k_j\}} \prod_j |r_X - r_A|^{-2x_{k_j}}
\end{aligned} \tag{II.3.4}$$

It is clear that the coefficients scale with $|r_X - r_A|^{\sum_j x_{k_j}}$. Now the correlators are computed independently, putting $r_X \to r_B$ and $|r_B - r_A| \to r$, the traces over the density matrices as present in the mutual information become

$$\frac{\operatorname{Tr}\rho^{(n)}_{A\cup B}}{\operatorname{Tr}\rho^{(n)}_A \operatorname{Tr}\rho^{(n)}_B} = \sum_{\{k_j\}} c^A_{\{k_j\}} c^B_{\{k_j\}} r^{-2\sum_j x_{k_j}}. \tag{II.3.5}$$

This expansion could be ordered to increasing scaling dimension, with the first term from the identity operator being of order unity, due to the one-point functions being 0 in the CFT. Inside the logarithm this term is unimportant and therefore the second contribution, of order $r^{-2(d-1)}$, is of interest.

II.3.2. Free Scalar Field Theory

Following the convention of using r for space coordinates in $\mathbb{R}^d$ and x for space-time coordinates in $\mathbb{R}^{d+1}$, the 2-point function and ϕ^2 - by means of point splitting - are written

$$\langle \phi(x_1)\phi(x_2)\rangle = G_0(x_2 - x_1) = |x_1 - x_2|^{-(d-1)} \tag{II.3.6a}$$

$$:\phi^2(x): = \lim_{\delta\to 0} \left(\phi(x + \tfrac{1}{2}\delta)\phi(x - \tfrac{1}{2}\delta) - G_0(\delta) \right) \tag{II.3.6b}$$

To compute the mutual information in the special case of a free scalar field theory, the trick is to find properly normalised local operators to put in the expansion. Cardy uses point splitting, Wick's theorem and the notion that one free field can be seen as n copies of fields on $\mathbb{R}^{d+1}$ with boundary conditions in A and B. Using flux conservation from the analogue in $d+1$ dimensional electrostatics he arrives at the leading correction of (II.3.5).

$$\frac{\operatorname{Tr}\rho_{A\cup B}^{(n)}}{\operatorname{Tr}\rho_A^{(n)}\operatorname{Tr}\rho_B^{(n)}} = \frac{1}{2}r^{-2(d-1)}n\Bigg[\lim_{x_1\to\infty}\sum_{j=0}^{n-1}x_1^{4(d-1)}\left(\left\langle\phi_j(x_1)\phi_0(x_1)\right\rangle_{C_A^{(n)}}\right)\left(\left\langle\phi_j(x_1)\phi_0(x_1)\right\rangle_{C_B^{(n)}}\right)+ \\ x_1^{4(d-1)}\left(\left\langle:\phi_0^2(x_1):\right\rangle_{C_A^{(n)}}\right)\left(\left\langle:\phi_0^2(x_1):\right\rangle_{C_B^{(n)}}\right)\Bigg] \tag{II.3.7}$$

Here $j'=0$ since there is a cyclic symmetry.

II.3.3. The case $n=2$

Define the linear combinations $\phi_\pm = 1/\sqrt{2}(\phi_0\pm\phi_1)$, which satisfy

$$\begin{aligned}\phi_-(r,0-) &= -\phi_-(r,0+) && (r\in A);\\ &= +\phi_-(r,0+) && (r\notin A),\\ \phi_+(r,0-) &= +\phi_+(r,0+) && \text{everywhere}\\ \left\langle\phi_\pm(x)\phi_\pm(x_1)\right\rangle &= \left\langle\phi_0(x)\phi_0(x)\pm\phi_1(x)\phi_0(x)\right\rangle.\end{aligned}$$

Again the correlators can be interpreted as the potential at x due to a unit charge at x_1. A useful choice is to let $x_1\to\infty$ along $A\cap(\tau=0)$, the symmetry of the potential under the reflection $\tau\to-\tau$ requires the potential to vanish. The hypersurface $A\cap(\tau=0)$ acts like a conductor at zero potential. For the far field, the field of interest, define

$$\begin{aligned}\bar\phi(x) &\equiv \left\langle\phi_-(x)\phi_-(x_1)\right\rangle - \left\langle\phi_+(x)\phi_+(x_1)\right\rangle\\ &= \left\langle\phi_-(x)\phi_-(x_1)\right\rangle - G_0(x-x_1),\end{aligned}$$

it is regular at x_1 and almost constant at $=|x_1|^{-(d-1)}$ on the conductor. The charge on the conductor then is $-\mathbf{C}_A|x_1|^{d-1}$, where $\mathbf{C}_A$ is the electrostatic capacitance. Taking $x, x_1\to\infty$ gives

$$\bar\phi(x) \sim -\mathbf{C}_A|x|^{-(d-1)}|x_1|^{-(d-1)} \tag{II.3.8a}$$

$$\left\langle\phi_1(x_1)\phi_0(x_1)\right\rangle \sim \tfrac{1}{2}\mathbf{C}_A|x_1|^{-2(d-1)} \tag{II.3.8b}$$

$$\left\langle:\phi_0^2(x_1):\right\rangle = \lim_{x\to x_1}\left(\left\langle\phi_0(x)\phi_0(x_1)\right\rangle - G_0(x-x_1)\right) = -\tfrac{1}{2}\mathbf{C}_A|x|^{-2(d-1)} \tag{II.3.8c}$$

$$I^{(2)}(A,B) \sim \frac{\mathbf{C}_A\mathbf{C}_B}{2r^{2(d-1)}} \tag{II.3.8d}$$

(II.3.8d) is valid for any compact regions A and B, but belonging coefficients are hard to come by. However for the special case of spherical $A\cap(\tau=0)$ the capacitance can be obtained.

Consider the oblate spheroid in $D = d + 1$ space-time defined by

$$\frac{r^2}{R_A^2} + \frac{x_D^2}{\lambda_D^2} = 1 \qquad \text{with} \qquad \lambda_D \ll R_A.$$

The starting point is a sphere with a uniform charge distribution that has zero field inside. Of course, this also holds for a shell with radii a and $a + \delta a$. Imagine acting with a shear transformation on the sphere $x'_j \to x_j = \lambda_j x'_j$ and the field components $E_j \to \lambda_j E_j = 0$, which ensure the remaining validity of Gauss' law. Since the bulk charge density, σ_0, between the shells is still uniform, in the limit $\delta a \to 0$, the surface charge density of a thin ellipsoid goes with the thickness of the ellipsoidal shell at x_j.

$$\sum_j x_j^2/\lambda_j^2 = a^2 \qquad \text{ellipsoid equation} \tag{II.3.9a}$$

$$\sum_j n_j dx_j = 0 \qquad \text{normal vector equation} \tag{II.3.9b}$$

$$n_j \propto \frac{x_j}{\lambda_j^2} \qquad \text{solution normal vecor} \tag{II.3.9c}$$

As will become clear, the bulk charge density can be a function of anything but r. If the bulk charge density is independent of r, it appears once in the numerator, via the total charge, and once in the denominator, via the potential. In particular we can define $\sigma_0(\lambda_D) = R_A/\lambda_D$. The surface charge density then becomes

$$\sigma(x) = \sigma_0(\lambda_D)\frac{\sum_j n_j x_j}{|n|} = \sigma_0(\lambda_D)\left(\sum_j \frac{x_j^2}{\lambda_j^4}\right)^{-1/2}. \tag{II.3.10}$$

Our ellipsoid is a specific one with $x_D = b\lambda_D$, a special dimension. The sphere is flattened along this dimension by letting $\lambda_D \to 0$. Note that in [7] $\lambda_D \to \infty$, this is assumed to be a typo. Furthermore, rescaling x_D gives the expression

$$\sum_{j=1}^{d} \frac{x_j^2}{R_A^2} = 1 - b^2,$$

where $|b| < 1$. Plugging everything in, the surface charge density becomes

$$\sigma(x) = \lim_{\lambda\to 0}\sigma_0(\lambda_D)\frac{1}{\sqrt{\frac{r^2}{R_A^2} + \frac{b^2}{\lambda_D^2}}} = \frac{R_A}{\lambda_D}\frac{\lambda_D}{|b|} = \frac{1}{\sqrt{R_A^2 - r^2}}. \tag{II.3.11}$$

The total charge and the potential are

$$Q = \int_0^a \frac{r^{d-1}}{\sqrt{R_A^2 - r^2}}dr = R_A^{d-1}\int_0^{\pi/2}(\sin(\theta)^{d-1}d\theta = R_A^{d-1}\frac{\Gamma(d/2)\Gamma(1/2)}{2\Gamma(d/2+1/2)};$$

$$V = \int_0^a \frac{r^{d-1}}{r^{d-1}\sqrt{R_A^2 - r^2}}dr = \int_0^{\pi/2} d\theta = \frac{\pi}{2}.$$

The capacitance is

$$\mathbf{C}_A = \frac{\Gamma(d/2)\Gamma(1/2)}{\pi\Gamma((d+1)/2)} R_A^{d-1}, \tag{II.3.12}$$

where $d+1=3$ gives Thomson's result, $\mathbf{C}_A = \frac{\pi}{2} R_A$, and $d+1=4$ gives $\mathbf{C}_A = \frac{1}{2} R_A^2$.

II.3.4. Free Field Theory with Spherical A and B for General n.

Up to now everything was valid for general regions, but to realise comparable results analytically, the conformal invariance in the case A and B are spheres is exploited. The mutual information then is a universal function of the following ratio of radii

$$I^{(n)}(A,B) = \frac{R_A R_B}{r^2 - (R_A - R_B)^2}.$$

The correlation functions transform covariantly under the type of mappings described in II.4. In particular the map that brings the hyper-surface ∂A that encloses A to an infinite plane, so that $A \cap \{\tau = 0\}$ is brought to a d-dimensional half-space, is of interest. The coefficients become

$$c^A_{jj'} = (2R_A)^{d-1} \left\langle \phi_j(1)\phi_{j'}(1) \right\rangle_{C^{\prime(n)}_A}.$$

Returning to the electrostatics analogue again, the potential on the jth copy at unit distance from the hyperplane that bounds A due to a unit charge in the same spot on the 0th copy is the desirable quantity. Switch to polar coordinates $(\rho, \theta, \vec{z})$, where ρ is along the axis of symmetry. The Green's function should satisfy $-\nabla^2 G^{(n)}(\rho,\theta,\vec{z}) \propto \delta(\rho-1)\delta(\theta)\delta^{d-1}(\vec{z})$. Now n initially was an integer, but suppose that it is $n = 1/m$, where m is an integer. Using the method of mirror images and setting $\rho = 1, \vec{z} = 0$ a solution can be found for all even $d-1$.

$$G^{(1/m)}(1,\theta,0) = \sum_{k=0}^{m-1} (2 - 2\cos(\theta + 2\pi k/m))^{-(d-1)/2} \tag{II.3.13}$$

The case $d = 3$

Of course the case $d=3$ is the one of interest and the power in the denominator becomes $(d-1)/2 = 1$. The solution is

$$G^{(1/m)}(1,\theta,0) = \sum_{k=0}^{m-1} (2 - 2\cos(\theta + 2\pi k/m)) = \frac{m^2}{2 - 2\cos m\theta}. \tag{II.3.14}$$

Note that a bit of a short cut was taken here, a regularisation using the limit $\rho \to 1-$ and some geometric series were involved to arrive at the rhs of (II.3.14), see [7]. Since originally not m, but n is supposed to be an integer, an analytical continuation, possible due to Carlson's theorem, is performed and

$$\left\langle : \phi_0^2(1) : \right\rangle = \lim_{\theta \to 0} \frac{1}{n^2} \left(\frac{1}{2 - 2\cos(\theta/n)} - \frac{n^2}{2 - 2\cos\theta} \right) = \frac{1 - n^2}{12 n^2}. \tag{II.3.15}$$

This gives the second term in (II.3.7), however for the limit $n \to 1$ the derivative vanishes. In other words it is a universal term contributing to the Renyi entropy, but not to the mutual information. Now look at the first term, the sum over the j copies of potentials of unit charges on the $d+1$ dimensional conifold. It can be evaluated to be

$$\sum_{j=1}^{n-1} G^{(n)}(1, 2\pi j/n, 0)^2 = \frac{1}{n^4} \sum_{j=1}^{n-1} \left(\frac{1}{2 - 2\cos(2\pi j/n)} \right)^2 = \frac{\left(n^2-1\right)\left(n^2+11\right)}{720 n^4} \tag{II.3.16}$$

Again some form of regularisation using $\rho \to 1-$, geometric series and Carlson's theorem allow the result for usage in an expression for the mutual information where the limit $n \to 1$ is taken. Now all building blocks for the computation of the mutual information are there. Summarising for $d = 3$

(II.3.1) $$I^{(n)}(A,B) = \frac{1}{n-1} \log \left(\frac{Z(C^{(n)}_{A\cup B}) Z^n}{Z(C^{(n)}_A) Z(C^{(n)}_B)} \right)$$

(II.3.5) $$\frac{\operatorname{Tr} \rho^{(n)}_{A\cup B}}{\operatorname{Tr} \rho^{(n)}_A \operatorname{Tr} \rho^{(n)}_B} = \sum \{k_j\} c^A_{\{k_j\}} c^B_{\{k_j\}} r^{-2\sum_j x_{k_j}}$$

(II.3.7) $$\frac{\operatorname{Tr} \rho^{(n)}_{A\cup B}}{\operatorname{Tr} \rho^{(n)}_A \operatorname{Tr} \rho^{(n)}_B} = \frac{n}{2r^4} \left[\lim_{x_1 \to \infty} \sum_{j=0}^{n-1} x_1^8 \left(\left\langle \phi_j(x_1) \phi_0(x_1) \right\rangle_{C^{(n)}_A} \right) \left(\left\langle \phi_j(x_1) \phi_0(x_1) \right\rangle_{C^{(n)}_B} \right) + \right.$$
$$\left. x_1^8 \left(\left\langle : \phi_0^2(x_1) : \right\rangle_{C^{(n)}_A} \right) \left(\left\langle : \phi_0^2(x_1) : \right\rangle_{C^{(n)}_B} \right) \right]$$

(II.3.15), (II.3.16) $$= \frac{n}{2r^4} \left(\frac{\left(n^2-1\right)\left(n^2+11\right)}{720 n^4} - \frac{\left(1-n^2\right)^2}{144 n^4} \right)$$

Remember that the coefficients $c^A_{jj'}$ are proportional to $(2R_A)^{(d-1)} = (2R_A)^2$ and that the lhs of eq. (II.3.7) is the leading term in eq. (II.3.5). The mutual information for general n then becomes

$$I^{(n)}(A,B) \sim \frac{n^4-1}{15 n^3 (n-1)} \left(\frac{R_A R_B}{r^2} \right)^2 .$$

Taking the derivative at $n = 1$ gives the mutual information.

$$\boxed{I(A,B) \sim \frac{4}{15} \left(\frac{R_A R_B}{r^2} \right)^2} \tag{II.3.17}$$

To summarise, this equation should be checked numerically. The problem is that the numerical methods available are based on spherical symmetry and an object consisting out of two spheres lacks such symmetry. To overcome this problem one can apply a conformal mapping which wraps one of the two spheres around the other in a concentric way.

II.4. Conformal Mapping

To use the results of II.3 for comparison with numerical results, some conformal mapping $f(x') : D' \mapsto D$ is necessary. The conformal mapping to use is an inversion around a point.

This transformation is a part of the more general Möbius transformation with the important property that it takes circles to circles and spheres to spheres.

Consider a $d+1$-dimensional space-time with a domain D' at $t=0$ were the numerical methods of chapter III are deployed. This domain can be divided in four regions, say A', B', C' and E', with concentric boundaries, see fig. 2. The three boundaries have radii r'_i, r'_o and r'_{ir}. Furthermore, note that the last boundary is not expected to play an important role when calculating entropies or the mutual information.

After the transformation , the spherical boundary at $x'_o = (r'_o, 0, \cdots, 0)$ is expected to be turned inside out. A new spherical region CE is created in the domain D. This way the result of [7], which describes the mutual information of region A with the combined region CE, can be written in terms of x'_i, x'_o and the uv-cutoff, provided that the distance between x_i and x_o is large enough.

A general inversion would look like

$$x^\mu = \frac{x^{\mu\prime} - y^{\mu\prime}}{(x' - y')^2}.$$

To define the transformation more precisely let

$$y' = (x'_p, 0, \cdots, 0),$$

and solely calculate the values for the 'x-axis' after inversion around this point. With the scaling factor, radius a, included, the inversion becomes

$$x = f(x') = a^2 \frac{x' - x'_P}{(x' - x'_p)^2} = \frac{a^2}{x' - x'_p}. \tag{II.4.1}$$

To apply the transformation to the inner sphere from 2a take the points (intersections of the spheres in 2b with the x-axis numbered from left to right)

$$\begin{aligned} x_1 &= \frac{a^2}{r'_i - x'_p} \quad \text{and} \quad x_2 = \frac{-a^2}{r'_i + x'_p}, \\ x_3 &= \frac{-a^2}{r'_o + x'_p} \quad \text{and} \quad x_6 = \frac{a^2}{r'_o - x'_p}. \end{aligned}$$

Region A and CE will become spheres of radii

$$\begin{aligned} r_i &= \frac{x_2 - x_1}{2} = \frac{a^2 r'_i}{x'^2_p - r'^2_i} \\ r_o &= \frac{x_6 - x_3}{2} = \frac{a^2 r'_o}{r'^2_o - x'^2_p} \end{aligned} \tag{II.4.2}$$

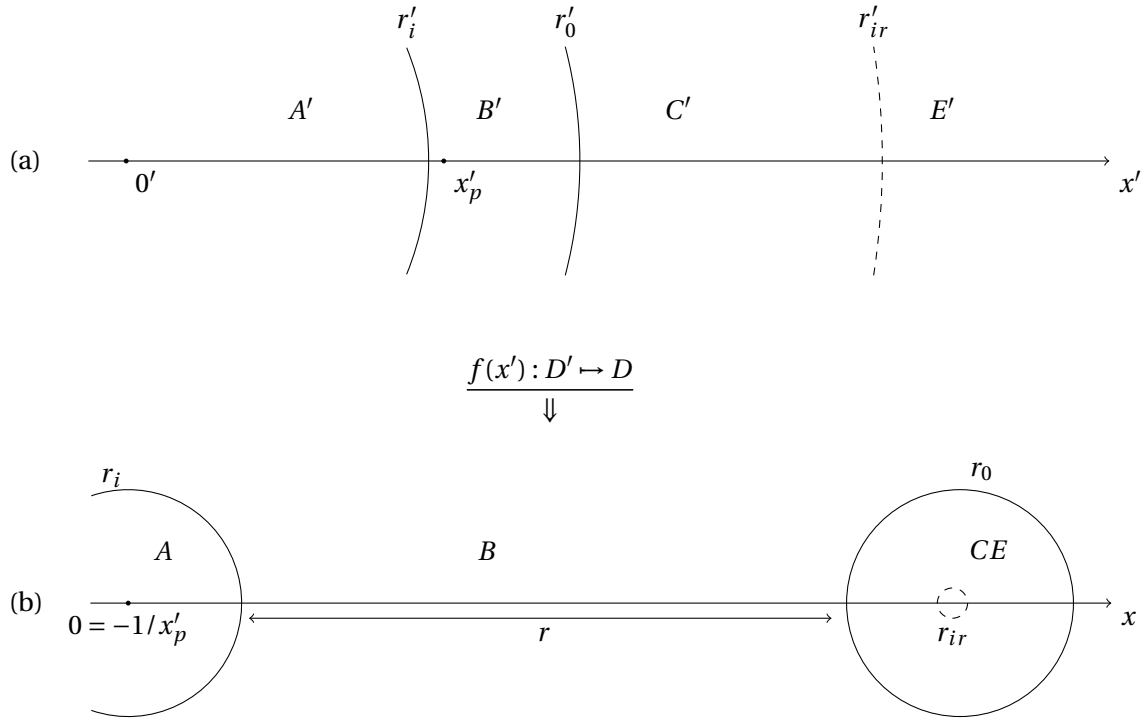

Figure 2: On the domain D' in fig. 2a the numerical methods of section IV.3 are applied and the methods of Cardy described in section II.3 are applicable on the domain D in fig. 2b .

respectively. Similarly the radius of the transformed IR-limit is

$$r_{ir} = \frac{a^2 r'_{ir}}{r'^2_{ir} - x'^2_P}.$$

Note that the spheres bordering regions C and E are not exactly concentric, but rather separated by a distance δ. Furthermore the application of II.3 requires the distance r to be large compared to the radii given above. These values are given by

$$\begin{aligned} \delta &= \frac{x_3 - x_4 - x_5 + x_6}{4} = \frac{a^2 x'_p \left(r'^2_{ir} - r'^2_o\right)}{\left(r'^2_o - x'^2_p\right)\left(r'^2_{ir} - x'^2_p\right)}; \\ r &= x_3 - x_2 = \frac{a^2 (r'_o - r'_i)}{(x'_p + r'_i)(x_p + r'_o)}. \end{aligned} \tag{II.4.3}$$

In the limit where $r'_i \to 0$ it is preferable to choose the value

$$x'_p = \sqrt{r'_i a},$$

so that region A has a radius $r_i \approx 1$ for $r'_i \to 0$. Substituting in equations II.4.2 and II.4.3 gives

$$\begin{aligned} r_i &= \frac{a^2}{a - r'_i} \approx a \\ r_o &= \frac{a^2 r'_o}{r'^2_o - r'_i a} \approx \frac{a^2}{r'_o} \\ \delta &= \frac{\sqrt{r'_i a^5}\left(r'^2_{ir} - r'^2_o\right)}{\left(r'^2_o - r'_i a\right)\left(r'^2_{ir} - r'_i a\right)} \approx \frac{\sqrt{r'_i a^5}(r'^2_{ir} - r'^2_o)}{r'^2_{ir} r'^2_o} \\ r &= \frac{a^2 (r'_o - r'_i)}{\left(\sqrt{r'_i a} + r'_i\right)\left(\sqrt{r'_i a} + r'_o\right)} \approx \sqrt{\frac{a^3}{r'_i}} \end{aligned} \tag{II.4.4}$$

Using these results the mutual information is written from II.3.17

$$I(A,B) \sim \frac{4}{15}\left(\frac{r_i r_o}{r^2}\right)^2. \tag{II.4.5}$$

Note that due to the universality of the mutual information a computation of it using conformally mapped regions is valid also. Expressed in the primed radii the mutual information becomes

$$I(A,B) \sim \frac{4}{15}\frac{r'^2_i}{r'^2_o}. \tag{II.4.6}$$

As it should, the scaling factor drops out of the the expression for the mutual information. However, looking forward to the numerical methods in chapter III, it is not expected that the limit $r'_i \to 0$ holds entirely. Therefore it is wise to plug in the mapped radii without the approximation. Also note that in this case the scaling factor can not take the values $a = n_i / n_o$

and $a = n_o/n_i$. The mutual information would blow up. It seems that the scaling factor plays a role in crude approximations. For the numerical chapter it is assumed to be $a = 1$. With the outer radius chosen to be $r'_o = 1$, the mutual information becomes a function of a ratio of the discretised radii n_i/n_o,

$$I(n_i, n_o) \sim \frac{4}{15}\left(\frac{\left(\sqrt{\frac{n_i}{n_o}} + \frac{n_i}{n_o}\right)^2 \left(\sqrt{\frac{n_i}{n_o}} + 1\right)^2}{\left(1 - \frac{n_i}{n_o}\right)^4}\right)^2 . \tag{II.4.7}$$

II.5. Review of 'Entropy and Area' by Srednicki

In this section the Srednicki method for numerical computation of entanglement entropy in QFT will be reviewed. We made some generalisations to allow for checking the mutual information numerically.

Putting in mind the notes on entropy, section II.1, Srednicki [6] starts with two coupled harmonic oscillators. The Hamiltonian, normalized ground state wave function and the density matrix are

$$H = \frac{1}{2}\left[p_1^2 + p_2^2 + \omega_+^2 x_+^2 + \omega_-^2 x_-^2\right] \tag{II.5.1a}$$

$$\psi(x_+, x_-) = \pi^{-1/2}(\omega_+\omega_-)^{1/4} \exp\left[-\tfrac{1}{2}(\omega_+ x_+^2 + \omega_- x_-^2)\right] \tag{II.5.1b}$$

$$\rho_o(x_2, x'_2) = \pi^{-1/2}(\gamma - \beta)^{1/2} \exp\left[-\gamma\tfrac{1}{2}(x_2^2 x_2'^2) + \beta x_2 x'_2\right] \tag{II.5.1c}$$

where

$$x_\pm = \frac{x_1 \pm x_2}{\sqrt{2}}\,, \qquad \omega_+ = \sqrt{k_0}\,, \qquad \omega_- = \sqrt{k_0 + 2k_1}\,,$$
$$\beta = \frac{(\omega_+ - \omega_-)^2}{4(\omega_+ + \omega_-)} \qquad \text{and} \qquad \gamma = \frac{8\omega_+\omega_- + (\omega_+ - \omega_-)^2}{4(\omega_+ + \omega_-)}\,.$$

The density matrix for the 'outer' oscillator, denoted by a subscript o, is found by tracing out the inner oscillator. By completing the square in the Gaussian integral, β and γ are found. From (II.1.1) the entropy, in terms of the eigenvalues p_n, is $S = -\sum_n p_n \log p_n$. To find these eigenvalues, solve

$$\int_{-\infty}^{\infty} dx' \rho_o(x, x') f_n(x'_n) = p_n f_n(x)\,. \tag{II.5.2}$$

The solution is obtained by meditation, magic, serendipity or simply 'guessing' the answer

$$\begin{aligned} p_n &= (1 - \xi)\xi^n \\ f_n(x) &= H_n(\alpha^{1/2} x) \exp[-\alpha x^2/2] \end{aligned} \tag{II.5.3}$$

where H_n is a Hermite polynomial,

$$\alpha = \sqrt{\omega_+\omega_-} \qquad \text{and} \qquad \xi = \frac{\beta}{\gamma - \alpha}\,.$$

Instead of two oscillators consider N coupled harmonic oscillators with Hamiltonian, normalized ground state wave function and density matrix

$$H = \frac{1}{2}\sum_{i=1}^{N} p_i^2 + \sum_{i,j=1}^{N} x_i K_{ij} x_j \tag{II.5.4a}$$

$$\psi_0(x_1,\cdots,x_N) = \left(\pi^{-N}\det\Omega\right)^{\frac{1}{4}} \exp\left[-x\cdot\Omega\cdot x/2\right] \tag{II.5.4b}$$

$$\rho_o(x_{n+1},\cdots,x_N;x'_{n+1},\cdots,x'_N) = \int\prod_{i=1}^{n} dx_i \psi_0(x_1,\cdots,x_N)\times\psi_0(x'_1,\cdots,x'_N) \tag{II.5.4c}$$

In (II.5.4a) K is a real symmetric matrix with positive eigenvalues. This means it is also diagonalizable. In (II.5.4b) Ω is the square root of K calculated by diagonalizing it and taking the square root of the diagonal terms. Note that in (II.5.4c) the product is taken over all first n to trace out and the completion of the square in the integral is carried out in a similar way as in the path integral of quantum field theory.

Then Ω is constructed by singular value decomposing K and the path laid out by Srednicki is to be continued. The square root matrix looks like

$$\Omega = \begin{pmatrix} A & B \\ B^T & C \end{pmatrix} \quad \text{where } A = n\times n \quad \text{and } C = (N-n)\times(N-n).$$

Since n components were traced out the other $N-n$ components remain.

Furthermore $\beta = B^T A^{-1} B$ and $\gamma = C - \beta = V^T\gamma_D V$, continuing diagonalisation with V orthogonal, giving

$$\rho_o(x,x') \sim \exp\left[-(x\cdot\gamma\cdot x + x'\cdot\gamma\cdot x')/2 + x\cdot\beta\cdot x'\right], \tag{II.5.5}$$

where $x = V^T\gamma_D^{-1/2}$ and $\beta' = \gamma^{-1/2}V\beta V^T\gamma_D^{-1/2}$. Set $y = Wz$, where like V, W is orthogonal, then $\beta'_D = W^T\beta' W$ and the density matrix can be written in terms of the eigenvalues of β',

$$\rho_o(z.z') \sim \prod_{i=n+1}^{N} \exp\left[\beta'_i z_i z'_i - (z_i^2 + z_i'^2)\right]. \tag{II.5.6}$$

Putting $\gamma \to 1$ and $\beta \to \beta'_i$ each term of $\rho(z,z')$ becomes identical to the density matrix from (II.5.1c). Letting

$$\xi_i = \frac{\beta'_i}{1+(1-\beta_i'^2)^{1/2}},$$

the total entropy becomes $S = \sum_i S(\xi_i)$, where the entropy terms are

$$S(\xi_i) = -\log(1-\xi_i) - \frac{\xi_i}{1-\xi_i}\log(\xi_i) \tag{II.5.7}$$

just as it would have been in the two oscillator case. Consider a quantum field with the Hamiltonian

$$H = \frac{1}{2}\int d^3\left[\pi^2(\vec{x}) + |\nabla\phi(\vec{x})|^2\right] \tag{II.5.8}$$

and introduce partial wave components

$$\begin{aligned}\phi_{lm} &= x\int d\Omega Z_{lm}(\theta,\psi)\phi(\vec{x})\,;\\ \pi_{lm} &= x\int d\Omega Z_{lm}(\theta,\psi)\pi(\vec{x})\,.\end{aligned} \tag{II.5.9}$$

Here the Z_{lm} are real spherical harmonics and the hermitian operators from (II.5.9) obey the commutation relation

$$\left[\phi_{lm}(x),\pi_{l'm'}(x')\right] = i\delta_{ll'}\delta_{mm'}\delta(x-x')\,.$$

The Hamiltonian in terms of these operators writes $H=\sum_{lm}H_{lm}$. Furthermore the radial coordinate x is replaced by a discrete lattice with spacing ν, giving an uv-cutoff $M=\nu^{-1}$. Similarly let the field vanish for $x\geq L=(N+1)\nu$, the ir-cutoff μ is thus L^{-1}. Putting the above together yields

$$H_{lm} = \frac{1}{2a}\sum_{j=1}^{N}\left[\pi^2_{lm,j}+(j+\frac{1}{2})^2\left(\frac{\phi_{lm,j}}{j}-\frac{\phi_{lm,j+1}}{j+1}\right)^2+\frac{l(l+1)}{j^2}\phi^2_{lm,j}\right]\,. \tag{II.5.10}$$

where $\phi_{lm,j}$ and $\pi_{lm,j}$ are dimensionless, hermitian, and obey the canonical commutation relation

$$\left[\phi_{lm,j},\pi_{l'm',j'}\right] = i\delta_{ll'}\delta_{mm'}\delta_{jj'}\,.$$

The partial Hamiltonian H_{lm} now has the form of (II.5.4a) and the entropy $S_{lm}(n,N)$ is calculated by tracing over the ground state of H_{lm} of the first n sites. Note that H_{lm} is independent of m, so that $S(n,N)=\sum_{lm}S_{lm}(n,N)=(2l+1)\sum_l S_l$. In the limit $l\gg N$ the l-dependent term in (II.5.10) dominates which leads perturbatively to a solution independent of N,

$$\begin{aligned}&S_l(n,N)=\xi_l\left[-\log\xi_l(n)+1\right]\\ &\text{where}\qquad \xi_l(n)=\frac{n(n+1)(2n+1)^2}{2^6l^2(l+1)^2}+O(l^{-6})\,.\end{aligned} \tag{II.5.11}$$

All in all the sum over l is convergent and enables a numerical calculation to check the area law of the entanglement entropy of a spherical region,

$$S=\frac{\alpha(1)}{\nu^2}R^2+\text{sub-leading}(R^2)\,,$$

where $R=\nu(n+b)$, ν is the uv-cutoff, b is any number in the interval $(0,1)$ and $\alpha(q)$ is some constant depending on the definition of entropy. Srednicki only uses the von Neumann entropy, $q=1$, but a generalisation is made to ensure consistency with [9] later on. In the next chapter, the arbitrary constant b is set to $1/2$ following Srednicki.

II.5.1. Generalisation to Arbitrary Concentric Region

Anticipating the extensions on the Srednicki calculations in appendix B, a note has to be made on the way the tracing is carried out. Since proving an area law was kept in mind in

the paper by Srednicki, the tracing was done over the n inner oscillators. However comparison with the results by Cardy described in II.3 urges to trace out a shell starting at some m and ending at $m+n$. This effect, however, is sorted easiest by using elementary row and column swapping operations on the matrix K, from eq. (II.5.4a), first.

Nota bene, at this point some remarks should also be made on the implications of this generalisation on the area law. Consider a thought experiment concerning the entropy of a more general spherically symmetric region, for example a shell with radii R_1 and R_2. When $R_1 \to 0$ it is expected that $S \propto R_2^2$, so a sphere with a cavity should also have a term scaling with R_2. On the other hand the area law is not expected to be valid just for spherically symmetric regions. For example, a half shell, or even a pierced shell, is also expected to have an entropy that depends on its area. But if the piercing of a shell is very thin, the entropy change due to this piercing is expected to contribute in a perturbative manner. The conclusion is that a shell, or more generally a spherically symmetric portion of space defined by a set of radii $\{R_i\}$, is expected to have an entropy proportional to

$$S(A,\bar{A}) \propto \sum_{i=1} R_i^2. \tag{II.5.12}$$

III

Methods

This chapter continues with an implementation of the results derived in II.5. To do this the numerical method sketched above, *Mathematica* was used. The scripts make use of the clever structure build in *Mathematica* that allows, or even encourages, the use of nested scripts. The first section, coupled to appendix A and appendix B, elucidates the code used to reproduce the results of [6] derived in the previous section. In the last paragraph the method is extended to any discrete spherically symmetric region using elementary matrix operations.

Thereafter, in sections III.2 and III.3 the overall structure of computation, data storage and graphical representation is made clear. As will become clear, the amount of time a machine consumes computing entropies on a discretised space with resolution $N = R_{\mathrm{IR}}/R_{\mathrm{UV}}$ scales with N^4. Therefore the choice for a structure with compact pre-computed data sets and lighter scripts to extract meaningful information appeared convenient. These two sections treat this issue and are coupled to appendix C and appendix D.

III.1. Entanglement Entropy on Spherical Lattice

The expression from eq. (II.5.7) is at the heart of the recipe. It is stated separately since one could in principle do the calculation for any definition of entropy, such as the more general Renyi entropy. This versatility comes in useful in the naturally preferred nested structure in *Mathematica*. This will become more clear in the next section.

As seen in line 5 of the code the uv-cutoff is set to one, making it the unit of length. The K matrix from II.5.1a is build in lines 6 to 9. Line 10 yields the first singular value decomposition which leads to the Ω matrix form in line 13. Lines 16 up to 20 cut Ω along the tracing boundaries, where after the linear algebra representing the completion of the square is applied. Then the second singular value decomposition takes place, giving the γ in II.5.5.

Here the reader should take a mental note regarding the singular value decompositions that are done. Theoretically they do not indicate something special, but most of the computing time is used doing them, especially for large values of the ir-cutoff. In the block consisting of lines 25 to 31 the eigenvalues are calculated and via the ξ_l's the contribution to the entan-

glement entropy for a particular l is evaluated.

To extend the functionality of script A.1 described above, such that it is possible to calculate entanglement entropies of more general sets of concentric regions in script B.1. one can simply swap rows and columns. Lines 17 to 32 do so, creating a redefined but not physically different Ω matrix. The partition of this matrix into A, B, B^T and C thereafter is the same.

III.2. Data Generation

It appeared that ad hoc computation of graphs similar to the ones in [6, 8] is not a workable option. It is not optimal to repeatedly compute singular value decompositions for every graph when the resolution gets larger. Long computation times, restricted RAM and variety in contemplated results demand a clear structure being used in the scripts for data generation.

As mentioned in the preamble of this chapter there is a steep scaling of computing time with the resolution, $T_{\text{comp}} \propto N^4$. The N^4 factor comes from the linear algebra used in the computation scheme. The number of equations solved in the singular value decomposition of the matrix K, that defines the Hamiltonian of the free field theory, approximately scales with N^3. Actually, this motivates the choice for *Mathematica* instead of another language, since *Mathematica* is expected to make good use of the fact that K is actually almost empty. Still, taking into account that the number of data points is proportional to N, the scaling power of the over all computation time is assumed to be at least 3 and could be close to 4.

To overcome the difficulties arising from this steep scaling of computation time with the resolution, during this research the ir-cutoff was held at twice the radius of the largest sphere in the calculation. However, it was shown in [8] that for low angular modes a higher ir-cutoff is needed to get a really good accuracy. They use an extrapolation method to calculate the entropies for low angular modes that unfortunately is beyond the scope of this research.

Keeping the above-mentioned in mind, some scripts were created to write calculated data to the hard disk and save RAM. One handles the most simple of regions, the sphere. It writes all results to the hard disk at once. The second, which calculates the entropy for various sets of shells, writes results in multiple files in a separate folder. Writing in multiple files while calculating does not only save RAM, but is also a safeguard for eventualities like power blackouts (really happened).

The first script, C.1, simply calculates the data needed to verify the area law for various definitions of the entropy. Input is: the ir-cutoff , the maximum radius of the sphere, the maximum value of the angular momentum and a parameter to distinguish between definitions of entropy. It simply sums over the angular momentum modes with the proper pre-factor due to a sum over m, see last part of II.5. The summed entropies are then stored together with their belonging radii.

The second, script C.2, is a bit more involved. Keep in mind that the entropy of region A is equal to that of the complementary region, $\bar{A}$. The entropy of a shell is thus equal to the entropy of the enclosed sphere together with the space outside. The option for in-script naming, taking into account the definition of entropy, is omitted as well as the option to set maximum angular momentum by hand. The latter is due to time preservation, the maximum

value of l is set to a minimum value being $2R_{\mathrm{IR}}$. It was checked that errors in the entropy using this ratio between R_{IR} and $l_{\max}$ were of the order of 1%. The fourth input of the function is a minimum distance between the outer and inner radius of the shell. It was assumed that numerical results using shells with a thickness of the order of the uv-cutoff are not reliable.

III.3. From Data to Results

The scripts in appendix D translate the raw data, usually labelled lists of entropies, into graphs and tables. Moreover, *Mathematica* provides some useful tools to fit functions and calculate meta-data. The stored files are imported in scripts D.1, D.2 and D.3. To save RAM and to gain speed, the latter two scripts should be nested in such a way that each data file is loaded once and all needed information is extracted.

Script D.1 represents affiliated data files, which are imported from the hard disk, together in one plot. It combines the results for computing the area law abiding entropies for different Renyi parameters q in one plot. Normally $q \neq 1$, but since it was shown in [6] that the limit $q \to 1$ is in fact the Neumann entropy, this case is treated similarly. Script D.1 also features the extraction of the coefficients that determine the area law-slope as a function of the Renyi parameter q. Script D.4 for example nests script D.3 in line 7 and uses the imported table to 3D-plot the entropies against the inner and outer radii of their belonging shells. Script D.5 nests both scripts D.2 and D.3 to give the mutual information of a sphere and a shell, with the ir-cutoff being the outer bound, numerically. It also nests script D.6, although it could also be used separately, which allows for comparison of the numerical mutual information with the analytical mutual information derived by Cardy. Basically, script D.6 computes all the parameters which define the conformal map, especially the distance between the to separate spherical regions.

As mentioned, *Mathematica* has some useful built-in functions to do fitting and collect meta-data given a set of data. Alike [8,9,16] the least squares fit method was used. The least squares method is the default fitting procedure for the functions `Fit` and `LinearModelFit`, which are built in functions in *Mathematica*.

IV

Results

The computations performed following the recipes described above gave some varying results. The first two sections of this chapter show that expected relations between the von Neumann entropy and area(s) of various regions are indeed reproducible using the numerics explained previously. In the first section the numerical factor of the area law, produced also by [8], is reproduced up to reasonable accuracy. The second section shows that the extension to arbitrary spherically symmetric regions using elementary matrix operation is valid and that it gives sensible results. The last section shows the results on the mutual information between a sphere and the rest of a space starting at a spherical boundary $R_{\text{out}} > R_{\text{sphere}}$. It also covers some parameters governing the conformal map and belonging comparison to the result of Cardy, see eqs. (II.4.4) and (II.4.5). In section V.1 the consequences of these parameters and their relation to the assumptions made in section II.3 are discussed more thoroughly.

The last section of this chapter starts somewhat similar to the first with the main difference being that the definitions of the entropy are set to the Renyi entropies with belonging parameters q, like in the computations in [9]. These use Renyi entropy definitions and also produce confirmation of the area law, be it with different coefficients. In this section these results are reproduced and the found relation between the Renyi-parameter q and the area law-coefficient $\alpha(q)$ is compared with the one in [9].

IV.1. Reproduction Area Law of a Sphere

The area law states that an entropy, in this case the von Neumann entropy ($q = 1$), is a function of $n^2 = (R/a + 1/2)^2$.

$$S(A, \bar{A}) = \alpha(q) n^2$$

In his paper Srednicki finds a value for the coefficient of proportionality of $\alpha(1) = 0.30$. The value found in [8] confirms that result and refines it to be $\alpha(1) = 0.2954$. The graph in fig. 3 was computed with the ir-cutoff set at $N = 60$ and for even values up to a maximum radius of $n = 30$ like in [6], it has a slope $\alpha(1) = 0.2952$.

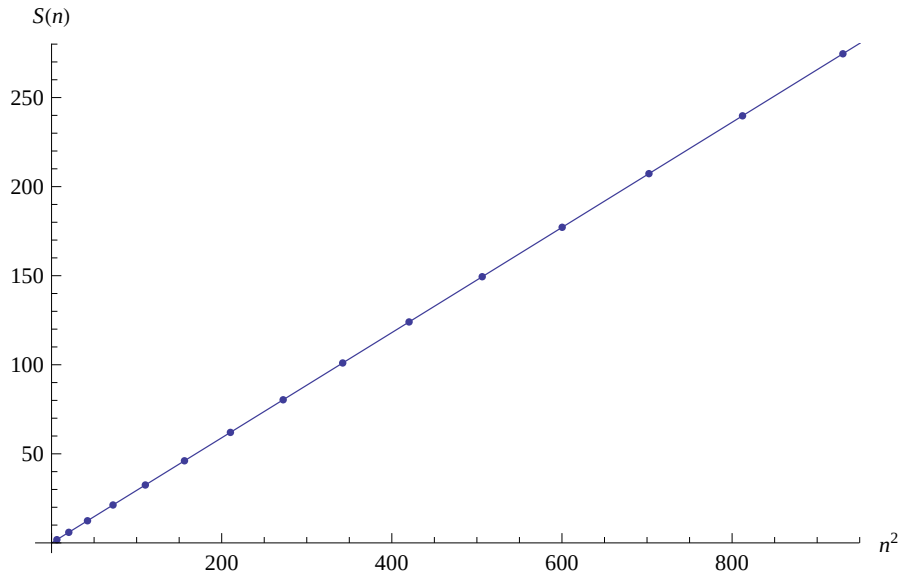

Figure 3: The entropy $S(n)$ resulting from tracing the ground state of a massless scalar field over the degrees of freedom inside a sphere of radius $n + 1/2$. The fitted function is $S(n) = -0.0439 + 0.2952\, n^2$. This graph should be considered a confirmation and an ode to the first numerical computation of the area law published in 1993 by Mark Srednicki.

IV.2. Area Law of other Concentric Regions

Recall eq. (II.5.12) and that it is expected that a shell defined by radii R_1 and R_2 has entropy

$$S(A,\bar{A}) = \frac{\beta(q)}{a^2}(R_1^2 + R_2^2) = \beta(q)(n_1^2 + n_2^2).$$

For the von Neumann entropy, following the procedure as described in section III.2, the entropy of a set of shells was computed. To produce fig. 4, the ir-cutoff was set to $N = 200$, the maximum radius of the outer shell was set to $n_{\max} = 99$, the minimum distance between the radii was set to $d_{\min} = 5$ and the minimum value of the inner radius was set to $n_{\min} = 10$.

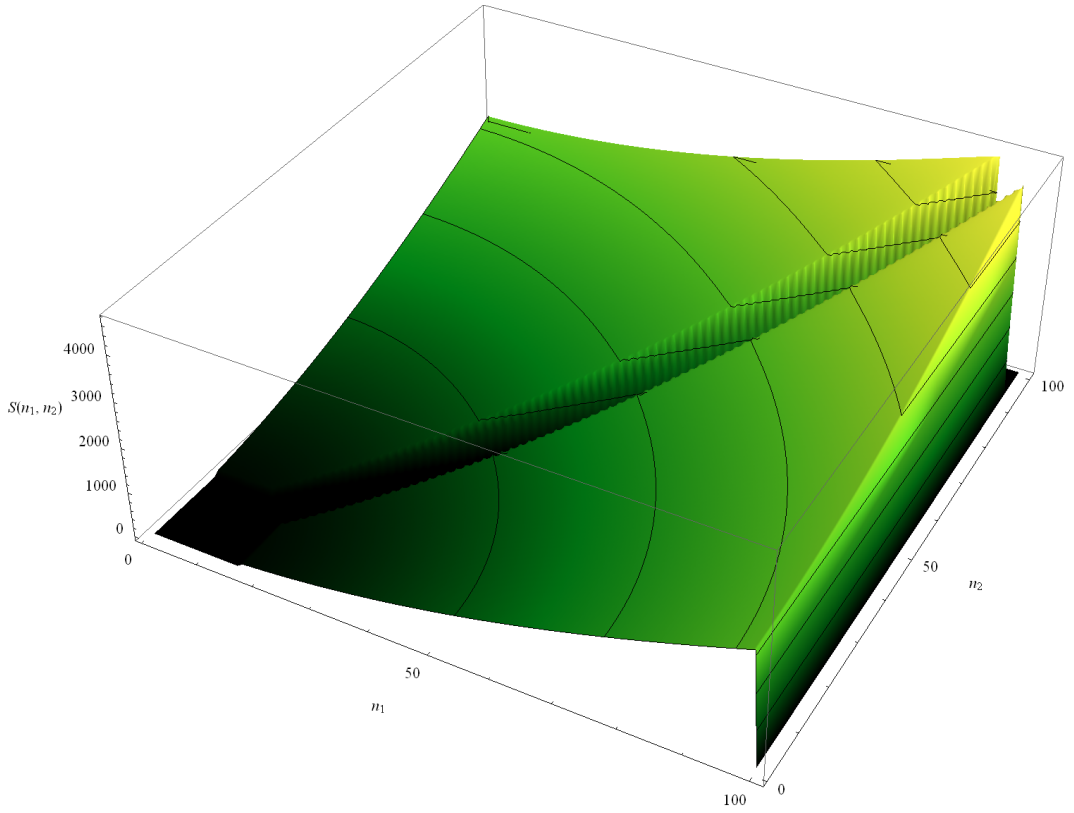

Figure 4: 3D-plot of the entropies of shells with varying inner and outer radii. The interpolation order is 1. For very thin shells no entropy was computed resulting in a gap along the diagonal of the plane spanned by n_1 and n_2. Note that half of the plot is obtained by mirroring the values in the other half, this is due to symmetry in $n_1 \leftrightarrow n_2$. The circular isohypses clearly visualise the expected area law for a spherically symmetric regions defined by two radii.

A surface fit of the data with and without constant was performed giving $S(n_1, n_2) = 48.2 + 0.257\left(n_1^2 + n_2^2\right)$ and $S(n_1, n_2) = 0.262\left(n_1^2 + n_2^2\right)$ respectively. The coefficients are of the same order as the area law coefficient in section IV.1. It is to be expected that more precise computations, that is using higher values for the ir-cutoff N and the maximum angular momentum

$l_{\max}$, result in the confirmation of the coefficient from [8] for general spherically symmetric regions, such as a shell.

IV.3. Mutual Information

Although the intended apotheosis of the numerical investigation appears bleak, some results on the mutual information of an inverse shell are tabulated below. The conformal mapping is simplified by the choices $x'_p = \sqrt{r'_i a}$ and $r'_o = 1$, see section V.1.

$r_i = n_i a = n_i / n_o$	$r_{i\text{-num}}$	r	$I_{\text{num}}(n_i, n_o)$	I_{C} [eq. (II.4.7)]	I_C [$\lim_{r\to\infty}$]
2/49	0.04082	3.286	0.01109	0.4027	$4.443 \cdot 10^{-4}$
2/39	0.05128	2.785	0.01432	0.5729	$7.013 \cdot 10^{-4}$
2/29	0.06896	2.224	0.01970	0.9331	$1.268 \cdot 10^{-4}$
2/19	0.1053	1.572	0.03061	2.022	$2.955 \cdot 10^{-3}$
5/49	0.1020	1.615	0.01109	1.903	$2.777 \cdot 10^{-3}$
5/39	0.1282	1.320	0.01432	3.020	$4.383 \cdot 10^{-3}$
5/29	0.1724	0.9951	0.01971	5.898	$7.927 \cdot 10^{-3}$
5/19	0.2632	0.6275	0.03067	18.71	$1.847 \cdot 10^{-2}$
10/49	0.2041	0.8359	0.01110	9.036	$1.111 \cdot 10^{-2}$
10/39	0.2564	0.6471	0.01433	17.27	$1.753 \cdot 10^{-2}$
10/29	0.3448	0.4429	0.01975	47.51	$3.171 \cdot 10^{-2}$
20/49	0.4082	0.3449	0.01112	96.00	$4.443 \cdot 10^{-2}$
20/39	0.5128	0.2310	0.01441	315.8	$7.013 \cdot 10^{-2}$

Table 1: Some results from computations of shell based mutual information. The first two columns on the left give the exact and numerical value of the parameter on which we expect the mutual information to depend. The third column lists the values of the distance between the spherical regions after a conformal mapping. The computed mutual information in column four is $I_{\text{num}}(n_i, n_o) = \nu^2 [S(n_i) + S(n_o) - S(n_i, n_o)]$. The factor ν^2 ensures $r'_o = 1$ for all values of n_i and n_o. Note that ν is not the same for all r_i. The last two columns state the predicted values using the calculated distance and infinite distance respectively.

The numerical mutual information in the fourth column below seems to depend on the value of the outer discretised radius, n_o, only. It is an unexpected result given the behaviour of the numerical outcome in sections IV.1 and IV.2. Though, it was expected that predicted values and numerical values do not match, given that the mapped distances which hardly approach infinity.

IV.4. Extension Area Law, Renyi Entropy

Contrary to the harvest of the previous section, good results were produced plugging in different entropy definitions. Building forth on section IV.1 the Renyi definition of entropy was implemented in the code giving various functions, $S^{(q)}(n)$, for the entropy. They are all area laws in leading order, that is $S^{(q)}(n) = \alpha(q)n^2 + \lambda(q)f(n)$, where $\lambda(q) \ll \alpha(q)$. Recall that q is the Renyi parameter, which leads to the von Neumann entropy when taking the limit $q \to 1$. It appears that the functions of entropy vary smoothly in q as is also found in [9].

The results presented in fig. 5 show the entropy functions that resulted from fitting the data with $S^{(q)}(n) = \text{constant} + \alpha(q)n^2 + \lambda(q)\ln n^2$. The plot that is set in besides the legend plots the area law coefficients versus the Renyi parameters. Like in Kim's article the fitted function is a polynomial of order 4 in $1/q$. It is hard to say what the precise relation between the area law coefficients and the Renyi parameters is.

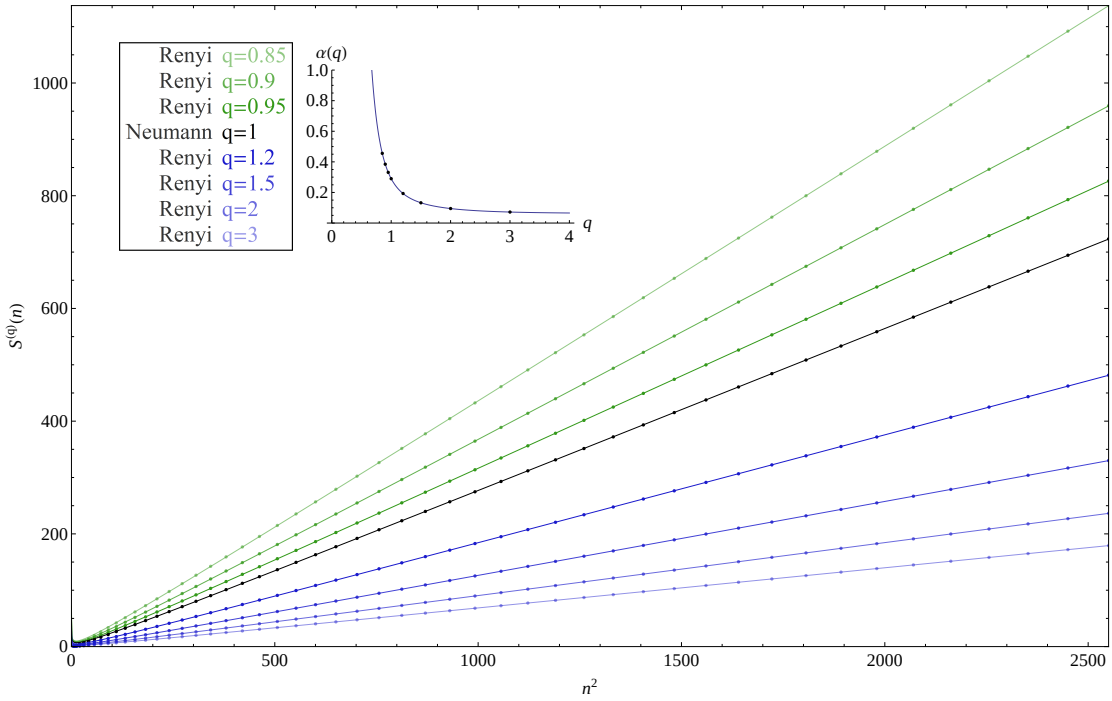

Figure 5: Entropies $S^{(q)}(n)$ for various values of q. The area law coefficients $\alpha(q)$ are plotted against the Renyi parameter in the plot next to the legend. The area law coefficients were obtained by fitting the entropy data with functions $S^{(q)}(n) = \text{constant} + \alpha(q)n^2 + \lambda(q)\ln n^2$. The logarithmic term differed from the term in [8] due to simplified computations on lower angular modes, see section III.2. Each entropy function was fitted through the last 40 data points. The area law coefficients in the top plot, as fitted to fourth order, gave $\alpha(q) = 0.0753 + 0.153\frac{1}{q} + 0.580\frac{1}{q^2} + 0.571\frac{1}{q^3} + 0.359\frac{1}{q^4}$.

V

Discussion

The results listed in the previous section cover a relatively narrow range of subjects, the neck of the hourglass. They cover free scalar field theory, embedded with spherical symmetry and except for section IV.4 only the von Neumann entropy definition. Section V.1 summarises these results and their consequences. Of course,when starting this investigation, an extended list of possible applications of the numerical methods used in this thesis came to mind. Putting in mass or some interaction are examples of further inquiry that are of interest. In section V.2 a synopsis of encountered pitfalls of this thesis is given. Special attention is paid to the relation between the resolution and computation time. Besides an evaluation on encountered dead ends and difficulties, the implications of this research on further investigations are dwelled upon. After swimmingly re-broadening the field of view, section I.1 is revisited in the last section of this chapter. Section V.3 attempts to find out how this piece relates to the puzzle.

V.1. Conclusions

The main conclusion of this research is that the computational framework based on [6] is very useful and easily adaptable for extended inquiries on entropy and mutual information. It was shown that for arbitrary spherically symmetric regions and definitions of entropy, sensible results are produced.

In section IV.1 it becomes clear that the famous area law is indeed reproduced with a sensible area law-coefficient of 0.2952. The fact that, even without the high N extrapolation on low angular modes, the result of [8] was reproduced differing only in the fourth digit, gives confidence.

The generalisation to arbitrary spherically symmetric regions using the script B.1 produced a good plot with aesthetically pleasing circular isohypses. Another confirmation of analytically predicted results. The area law does not only hold for spheres, but for a wider range of geometrical regions.

In section IV.3 the numerical mutual information is listed giving slightly odd results. It was

computed using

$$I_{\text{num}}(n_i, n_o) = v^2 \left[S(n_i) + S(n_o) - S(n_i, n_o) \right],$$

where the entropies are similar to the entropies in sections IV.1 and IV.2. From looking at this formula or scripts B.1 and C.2, it is hard to explain why the mutual information should only depend on the value of the discretised outer radius, n_o. From the limited data produced it is also hard to conclude whether the numerical mutual information converges to the predicted value from the Cardy paper.

Section IV.4 shows that the expansion of methods using different definitions of entropy still obeys the area law. It is expected that a further generalisation, for example the arbitrary concentric region case, will not give essentially different results when using a definition of entropy different from the von Neumann entropy. The area law coefficients $\alpha(q)$ seem to scale as a polynomial of $1/q$, but no elegant area law coefficient law appeared. The results obtained were very similar to the results by Kim in [9].

V.2. Evaluation and Recommendations

The preconditions of this research were, 1 undergraduate, 1 year, 1 personal computer (containing a 3 GHz processor and 4 Gb RAM). Within this volume in facility space it was possible to reproduce most results in similar research, but a good leap forward appeared out of grasp. What would it need to check Cardy's result numerically? The scaling of computation time with the resolution to a power of four, mentioned in chapter III, is a hurdle which can only be jumped extending this volume in all directions. Let us evaluate all axes of facility space and see what possible issues arise and how they are to be solved.

Firstly focus on the undergraduate. Assuming the student follows the quantum universe master of the Rijksuniversiteit Groningen, a few months of the available year need to be spend studying GR, AdS/CFT and Conformal since courses in the curriculum only scratch the surface of these topics. Besides that, some time is also lost familiarising with *Mathematica* and the numerics involved in a research. Results also need to be put on paper, leaving approximately 3 months worth of computation time to produce results. Moreover, further research might require the computational methods in *Mathematica* to be revised for efficient computation. That might bring the scaling of computation time down. This can not be expected of a physics undergraduate. It is recommended that a serious attempt to reproduce Cardy's result is carried out by graduates with a good basis in the topics mentioned and a thorough understanding of numerical methods. Further conduction by an undergraduate should focus on one of the extensions proposed in the preamble of this chapter.

Secondly take a look at the time aspect. It is not unrelated to occupation of the investigatives. Since a large part of the time of research is consumed purely by computation, it is wise to conduct it besides other activities. Remember that, to get credible results, the resolution needs to be scaled with a factor of order 10^3. Due to the relation $T(n) \propto n^p$ were $3 < p < 4$ this results in millions of years of computation of a personal computer. Lets assume that a realistic time scale for any research is maximally ~ 10 year. Some fundamentally different kind of computing power is needed too.

Luckily, due to Moore's law, the third direction of facility space is travelled exponentially. Assuming smart numerics bringing p down to 3 and $T_{max} \sim 10$ year, we need to amp our computing power by a factor of 10^7. The best supercomputers in the world manage about 30 PFLOPS, $10^{6.5}$ times faster than a personal computer.

When attempted seriously by a good team of scientists and programmers, the basic methods in this research are enabling the intended comparison with Cardy's result.

V.2.1. Some Philosophy of Science

Note that in modern frontier physics there a basically four ways to learn more about the universe. One can analytically build upon earlier results, one can look into space, one can do a high energy experiment or one can simulate a process. Usually a theory gains a lot of credibility if it can be verified by multiple methods.

An important comment on the first method could be that, for a theory beyond the present measurement scale, based on other theories which are not, to be valid, it should at least verify those theories on the scales they were measured. In the case of a quantum gravity description of a black hole evaporation process this would mean that the horizon should indeed be smooth.

When the results appearing from the first method are not verifiable from space observations, two options are left. Sadly, the third method nowadays is running against its boundaries. Due to the fact that computer simulations still seem to have Moore's law on their side, one expects them to play an even bigger role in strengthening analytical results in the future.

V.3. The Bigger Picture

Reviewing the discussion treated in chapter I, it would be interesting to find out where to add this piece, detailed numerical research as discussed in this thesis, in the puzzle that is the black hole information problem. Up to now no theoretical framework has successfully passed the all important test of black hole creation and evaporation. The black hole complementarity principle for example looks very promising from an intuitive philosophical point, but it has to be made precise to contribute to physics.

It would be nice to see whether the introduction of curved backgrounds, non-trivial entanglement structures or non-scalar fields change the quantitative behaviour of the entropy along region boundaries. Is the area law still valid in these cases? Are there more hints on how the holography principle effects our universe to be found in detailed research of entanglement entropies?

It is clear that this thesis is not answering all of these questions. However, the limited amount of articles to be found on such a beautiful and essential topic as entropy numerics motivates a serious pick up of the baton left here for the next stage.

Bibliography

[1] S. W. Hawking, "Breakdown of predictability in gravitational collapse," *Phys. Rev.* **D14** (1976) .

[2] L. Susskind and L. Thorlacius, "Gedanken experiments involving black holes," arXiv:hep-th/9308100 [hep-th].

[3] S. D. Mathur, "Fuzzballs and black hole thermodynamics," arXiv:hep-th/1401.4097v1 [hep-th].

[4] J. P. Ahmed Almheiri, Donald Marolf and J. Sully, "Black holes: Complementarity or firewalls?," arXiv:hep-th/1207.3123v4 [hep-th].

[5] S. D. Mathur, "Remnants, fuzzballs or wormholes?," arXiv:1406.0807v1 [hep-th].

[6] M. Srednicki, "On entropy and area," arxiv:hep-th/9303048v2 [hep-th].

[7] J. Cardy, "Some results on mutual information of disjoint regions in higher dimensions," arXiv:1304.7985v3 [hep-th].

[8] A. S. R. Lohmayer, H. Neuberger and S. Theisen, "Numerical determination of entanglement entropy for a sphere," arXiv:0911.4283v1 [hep-th].

[9] N. Kim, "On numerical calculation of renyi entropy for a sphere," *Physical Letters B* (2014) .

[10] J. Preskill and P. Schwarz, "Limitations on the statistical description of black holes,".

[11] M. C. J. Sean M. Carroll and L. Randall, "Extremal limits and black hole entropy," arXiv:0901.0931v2 [hep-th].

[12] T. Jacobson, "Thermodynamics of spacetime: The einstein equation of state," arXiv:gr-qc/9504004v2 [hep-th].

[13] N. Shiba, "Entanglement entropy of two spheres," arXiv:1201.4865v4 [hep-th].

[14] C. Callan and F. Wilczek, "On geometric entropy," arXiv:9401072 [hep-th].

[15] S. G. S. Santosh Kumar and S. Shankaranarayanan, "Entanglement entropy for nonzero genus topologies," arXiv:1401.2839v2 [hep-th].

[16] L. M. Jeongseog Lee and B. R. Safdi, "Renyi entropy and geometry," arXiv:1403.1580v2 [hep-th].

[17] Y. Nakaguchi and T. Nishioka, "Entaglement entropy of annulus in three dimensions," arXiv:1501.01293v1 [hep-th].

[18] V. Vedral, "The role of relative entropy in quantum information theory," arXiv:quant-ph/0102094v1 [hep-th].

[19] J. Steinbeck, *Once there was a war*. 1958.

[20] H. V. Youngjai Kiem and E. Verlinde, "Black hole horizons and complementarity," arXiv:hep-th/9502074v2 [hep-th].

[21] L. Susskind and J. Lindesay, *An introduction to black holes, information and the string theory revolution: The Holographic Universe*. 2005.

[22] S. W. Hawking, "Black hole explosions," *Nature* (1974) .

[23] S. W. Hawking, "Particle creation by black holes," *Commun. Math. Phys.* (1975) .

[24] J. D. Bekenstein, "Black holes and entropy," *Physical Review D* (1973) .

[25] G. 't Hooft, "On the quantum structure of a black hole," *Nuclear Physics* (1984) .

[26] P. Hayden and J. Preskill, "Black holes as mirrors: quantum information in random subsystems," arXiv:0708.4025v2 [hep-th].

[27] Y. Sekino and L. Susskind, "Fast scramblers," arXiv:0808.2096v1 [hep-th].

[28] K. P. Jan de Boer and E. Verlinde, "Black hole berry phase," arXiv:0809.5062v1 [hep-th].

[29] S. D. Mathur, "What does strong subadditivity tell us about black holes?," arXiv:hep-th/1309.6583 [hep-th].

[30] K. Papadodimas and S. Raju, "An infalling observer in ads/cft," arXiv:1211.6767v1 [hep-th].

[31] S. G. Avery, "Qubit models of black hole evaporation," arXiv:1109.2911v2 [hep-th].

[32] P. Calabrese and J. Cardy, "Entanglement entropy and quantum field theory," arXiv:0405152 [hep-th].

[33] J. C. Pasquale Calabrese and E. Tonni, "Entanglement entropy of two disjoint intervals in conformal field theory," arXiv:0905.2069v2 [hep-th].

[34] C. E. Shannon, "A mathematical theory for comunnication," *New York: Interscience* (1948) .

[35] H. Casini and M. Huerta, "Entanglement entropy in a free quantum field theory," arXiv:0905.2562v3 [hep-th].

A

Reproducing Area Law Srednicki

In this appendix the article by Srednicki, is translated to code. The first script sets the definition of the entropy, which is set to the von Neumann entropy in this case following Srednicki. However, for more generalised results the Renyi entropy can also be used. It is not shown explicitly in code, but just altering the entropy in the script below allows reusing all the nested scripts in this appendix. NB: It is wise to change the parent directory also, since new results, with another definition of entropy, could replace old results.

Script A.1 Definitions

```
renn = 1;
If[renn == 1, s[x_] := -Log[1 - x] - x/(1 - x) Log[x];
  , s[x_] := -1/(1 - renn) Log[(1 - x)^renn/(1 - x^renn)];]
pardir = "c:\\Users\\Ernst␣\
Stam\\Documents\\Studie\\Scriptie\\Mathematica\\Data";
SetDirectory[pardir]
(* Define the entropy and set the working directory for convenience.
    *)
```

The code below translates the recipe from [6] to Mathematica code.

Script A.2 Srednicki

```
S[NN_Integer, n_Integer, l_Integer] := Module[{uvc, K1, left, kd,
    right, skd, Omega, A, B, CC, beta, gamma.leftg.diagonalg, rightg,
    gammd.betap.eigenbetap, xis, EE},

 uvc = 1.; (*The uv-cutoff is set to one for simplicity.*)
 K1 = 1/uvc Table[ KroneckerDelta[i, j] ((j + 1/2)^2/j^2 + (j - 1/2)
     ^2/(j^2) + l (l + 1)/j^2) - KroneckerDelta[i, 1] KroneckerDelta[
```

```
    j, 1] 1/4 - 2 KroneckerDelta[j + 1, i] (j + 1/2)^2 (1/j/(j + 1))
    , {i, 1, NN}, {j, 1, NN}];
 K = (K1 + Transpose[K1])/2;
 {left, kd, right} = SingularValueDecomposition[K];
 skd = Table[ KroneckerDelta[i, j] Sqrt[kd[[i, j]]], {i, 1, NN}, {j,
    1, NN}];
 Omega = left.skd.Transpose[right];
 (*Definition of the Hamiltonian matrix and taking the square root*)

 A = Table[Omega[[i, j]], {i, 1, n}, {j, 1, n}];
 B = Table[Omega[[i, j]], {i, 1, n}, {j, n + 1, NN}];
 CC = Table[Omega[[i, j]], {i, n + 1, NN}, {j, n + 1, NN}];
 beta = 1/2 Transpose[B].Inverse[A].B;
 gamma = CC - beta;
 {leftg, diagonalg, rightg} = SingularValueDecomposition[gamma];
 gammd = Table[KroneckerDelta[i, j] Sqrt[diagonalg[[i, j]]], {i, 1,
    NN - n}, {j, 1, NN - n}];
 (*Generalized procedure of tracing and 'completing the square'*)

 betap = Inverse[gammd].Transpose[rightg].beta.leftg.Inverse[gammd];
 eigenbetap = Eigenvalues[betap];
 Do[If[eigenbetap[[i]] == 0, eigenbetap[[i]] = 10^(-150)], {i, Length
    [eigenbetap]}];
 xis = Table[ eigenbetap[[i]]/(1 + Sqrt[1 - eigenbetap[[i]]^2]), {i,
    1, NN - n}];
 EE = Sum[s[xis[[i]]], {i, 1, NN - n}]
 (*Calculating entaglement entropy for a specific l and m mode*)
]
```

B

Extension to General Concentric Regions

The code below effectively does the same thing as the one from appendix A. What makes it an extension, lies in the fact that the matrix from the Hamiltonian is 'shuffled' before acting with the tracing procedure. Some attention goes to the fact that in the case of an even amount of input parameters, the inside sphere is not traced over. This is due to the necessity of leaving the most outer region untraced for validity of the procedure.

Script B.1 Generalisation to arbitrary set of spherically symmetric regions

```
S[NN_Integer, n__Integer, l_Integer] := (
 uvc = 1.;
 P = Sort[{1, n, NN}, Less];
 lp = Length[P];
 ball = Mod[lp, 2];
 bip = 2 - Mod[lp, 2];
 bop = 1 + Mod[lp, 2];
 (*Due to the variable amount of input parameters, some extra
    definitions where made to slender the code a bit*)

 K1 = 1/uvc Table[
  KroneckerDelta[i, j] ((j + 1/2)^2/j^2 + (j - 1/2)^2/(j^2) + l (l +
      1)/j^2) -
  KroneckerDelta[i, 1] KroneckerDelta[j, 1] 1/4 - 2 KroneckerDelta[j
      + 1, i] (j + 1/2)^2
   (1/j/(j + 1)), {i, 1, NN}, {j, 1, NN}];
 K = (K1 + Transpose[K1])/2;
 (*The matrix is build just as before.*)

 If[Length[P] > 3, {lc = (Length[P] - ball)/2 - 1;
  Do[
   mm = K[[ P[[2 i + ball]] ;; P[[2 i + ball + 1]] - 1]];
   K = Drop[K, {P[[2 i + ball]], P[[2 i + ball + 1]] - 1}];
   Do[
```

```
      K = Insert[K, mm[[j]], P[[i]] + j - 1],
    {j, 1, Dimensions[mm][[1]]}];
    K = Transpose[K];
    mm = K[[ P[[2 i + ball]] ;; P[[2 i + ball + 1]] - 1]];
    K = Drop[K, {P[[2 i + ball]], P[[2 i + ball + 1]] - 1}];
    Do[
      K = Insert[K, mm[[j]], P[[i]] + j - 1],
    {j, 1, Dimensions[mm][[1]]}];
    K = Transpose[K];
  , {i, 1, lc}]
}];
(* Elementary matrix operations 'line up' the parts that are traced
   over.*)

{left, kd, right} = SingularValueDecomposition[K];
skd = Table[
  KroneckerDelta[i, j] Sqrt[kd[[i, j]]], {i, 1, NN}, {j, 1, NN}];
Omega = left.skd.Transpose[left];

nn = Sum[P[[i + 1]] - P[[i]], {i, bip, lp - 1, 2}];
A = Table[Omega[[i, j]], {i, 1, nn}, {j, 1, nn}];
B = Table[Omega[[i, j]], {i, 1, nn}, {j, nn + 1, NN}];
CC = Table[Omega[[i, j]], {i, nn + 1, NN}, {j, nn + 1, NN}];
beta = 1/2 Transpose[B].Inverse[A].B;
gamma = CC - beta;
{leftg, diagonalg, rightg} = SingularValueDecomposition[gamma];
gammd = Table[
  KroneckerDelta[i, j] Sqrt[diagonalg[[i, j]]], {i, 1, NN - nn}, {j,
     1, NN - nn}];

betap = Inverse[gammd].Transpose[rightg].beta.leftg.Inverse[gammd];
eigenbetap = Eigenvalues[betap];
Do[
  If[eigenbetap[[i]] == 0, {
    eigenbetap[[i]] = 10^(-150);
    q = {{{n}[[1]]}, {{n}[[2]]}, {1}};
    meta = ArrayFlatten[{{meta, q }}]
  }],
{i, Length[eigenbetap]}];
xis = Table[
  eigenbetap[[i]]/(1 + Sqrt[1 - eigenbetap[[i]]^2]), {i, 1, NN - nn
     }];
EE = Sum[s[xis[[i]]], {i, 1, NN - nn}]
(*For the details of the rest of the code see Appendix A.*)
)
```

C

Generating Data

For a particular definition of the entropy, the entropies for a range of radii are tabulated together with the values of $R^2 \equiv (r+1/2)^2$, in units of the uv-cutoff.

Script C.1 Generate data set for a sphere

```
arealaw[NN_, nmax_, ang_, s_] := Module[{datasp, l, j, name},
 If[s == 1, name = "Neumann", name = "Renyi"];
 datasp = Table[{(j+1/2)^2,Sum[(2 l + 1) S[NN, j, l], {l, 0, ang}]},
     {j, nmax}];
 Export["EE-" <> name <> "-" ToString[NN] <> "-" <> ToString[nmax] <>
     "-" <> ToString[ang] <> ".dat", datasp];
]
```

The next script was designed with the comparison to Cardy's formula, (II.4.5). The input consists of the ir-cutoff, the minimum value of the outer radius, the maximum value of the outer radius and a minimum thickness for the shell. In line 5 there is a `For` loop running over all outer radii that produces, for every term, a table that is written to a separate file. These tables then run over all values that the inner radius can take, keeping in mind the minimal thickness of the shell. Line 11 then creates another table containing the entropies of spheres with radii running up to $R_{\max}$. Together these files are stored in a folder which is labelled with the ir-cutoff and the minimum thickness of the shells.

Script C.2 Generate data set for a shell and enclosed sphere

```
1 datagen[NN_, nmin_, nmax_, dmin_] := Module[{ll, ii, k, l, rout,
    datash, datasp},
2  CreateDirectory["datagen-" <> ToString[NN] <> "-" <> ToString[dmin
     ]];
3  SetDirectory[pardir <> "\\datagen-" <> ToString[NN] <> "-" <>
     ToString[dmin]];
4  Monitor[
5    For[rout = nmin + dmin + 2, rout < nmax + 1, rout++,
6     datash = Table[ S[NN, ii, rout, ll], {ll, 0, 2 NN}, {ii, 2, rout
        - dmin}];
7     Export["EE-sh-" <> ToString[NN] <> "-" <> ToString[nmin] <> "-"
        <> ToString[nmax] <> "-" <> ToString[dmin]
8       <> "-" <> ToString[rout] <> ".dat", datash];
9       ]
10 , {ll, ii, rout}];
11   Monitor[datasp = Table[ S[NN, k, l], {k, 2, nmax}, {l, 0, 2 NN}],
       l];
12   Export["EE-sp-" <> ToString[NN] <> "-" <> ToString[nmax] <> ".dat"
       , datasp];
13   SetDirectory[pardir];
14 ]
```

D

Handling Data

It is important to note that 3 types of data were created. The first type, scripts C.1, D.1 and D.2, allows for checks of the area law in [6] and consists of entropies of spherical regions only. The second type, scripts C.2, D.2 and D.3, is grouped data consisting of entropies of spherical and shell-like regions in one folder labelled by the conditions (ir-cutoff, minimal thickness of shell, starting value outer radius) under which they were computed.

Script D.1 Import data and produce graph

```
impee[NN_, l_, step_] := Module[{fn, dat, i, d, dats, data, fit, lp,
    fp, graph},
 fn = "ee" <> ToString[NN] <> ToString[l] <> ToString[step] <> ".dat"
     ;
 Print[fn];
 dat = Transpose[Import[fn, "Table"]];
 d = Dimensions[dat][[2]];
 dat[[1]] = N[ToExpression[dat[[1]] ]];
 dats = {N[dat[[2]]/dat[[1]]], N[dat[[2]]/dat[[1]]]};
 dats = ArrayFlatten[{{dat}, {dats}}];
 data = dats[[1 ;; 3]];
 Print[Grid[data, Frame -> True]];
 fit = LinearModelFit[Transpose[data[[1 ;; 2]]], {1, n}, n];
 lp = ListPlot[Transpose[data[[1 ;; 2]]], AxesLabel -> {n^2, S[n]}];
 fp = Plot[fit[n], {n, 0, 1000}];
 Print[Normal[fit]];
 graph = Show[lp, fp, Frame -> True];
 Export["ee" <> ToString[NN] <> ToString[l] <> ToString[step] <> ".
     pdf", graph];
 Print[graph];
 ]
```

This script in essence is similar to script D.1, but a lot of code is needed to lay out a multiple line graph. The last input parameter `s_List` should be a list of the values of q for which the entropies were computed.

Script D.2 Check area law for different definitions of entropy

```
areaimp[NN_Integer, nmax_Integer, ang_Integer, fl_Integer, s_List] :=
    Module[{st, m, datasp, l, j, name, data, fitdata, fit, color,
   graph, lp, fpsl, max, ff, coeff, rr, pc, legend, plot},

 st = Sort[s, Less];
 data = s;
 fit = s;
 color = s;
 graph = s;
 coeff = s;
 fpsl = s;
 m = Count[st, u_ /; u > 1];
 l = Count[st, u_ /; u < 1];

 Do[
  If[st[[i]] == 1, name = "Neumann";
   datasp = Import["EE-" <> name <> "-" <> ToString[NN] <> "-" <>
      ToString[nmax] <> "-" <> ToString[ang] <> ".dat", "Table"];
   datasp[[All, 1]] = N[ToExpression[datasp[[All, 1]]]];
   fitdata = datasp[[-fl ;; -1]];
   ff = LinearModelFit[fitdata, {1, Log[x], x}, x];
   coeff[[i]] = {st[[i]], ff[[1, 2, 3]]};
   fit[[i]] = {Normal[ff]};
   data[[i]] = datasp;
   color[[i]] = Black;
   graph[[i]] = {Style["Neumann", FontColor -> RGBColor[.2, .2, .2],
       FontFamily -> "Times", FontSize -> 20], Style["q=" <>
      ToString[st[[i]]], FontColor -> color[[i]], FontFamily -> "
      Times", FontSize -> 20]},
   name = "Renyi-" <> ToString[st[[i]]];
   If[st[[i]] < 1,
    datasp = Import["EE-" <> name <> "-" <> ToString[NN] <> "-" <>
       ToString[nmax] <> "-" <> ToString[ang] <> ".dat", "Table"];
    datasp[[All, 1]] = N[ToExpression[datasp[[All, 1]]]];
    fitdata = datasp[[-fl ;; -1]];
    ff = LinearModelFit[fitdata, {1, Log[x], x}, x];
    coeff[[i]] = {st[[i]], ff[[1, 2, 3]]};
    fit[[i]] = {Normal[ff]};
    data[[i]] = datasp;
    color[[i]] = RGBColor[0.2, .6, .1, .3 + .7 i/l];
    graph[[i]] = {Style["Renyi", FontColor -> RGBColor[.2, .2, .2],
       FontFamily -> "Times", FontSize -> 20], Style["q=" <>
      ToString[st[[i]]], FontColor -> color[[i]], FontFamily -> "
      Times", FontSize -> 20]},
```

```
35
36      datasp = Import["EE-" <> name <> "-" <> ToString[NN] <> "-" <>
            ToString[nmax] <> "-" <> ToString[ang] <> ".dat", "Table"];
37      datasp[[All, 1]] = N[ToExpression[datasp[[All, 1]]]];
38      fitdata = datasp[[-fl ;; -1]];
39      ff = LinearModelFit[fitdata, {1, Log[x], x}, x];
40      coeff[[i]] = {st[[i]], ff[[1, 2, 3]]};
41      fit[[i]] = {Normal[ff]};
42      data[[i]] = datasp;
43      color[[i]] = RGBColor[.1, .1, .8, .3 + .7 (m - i + 1 + 2)/(
            Length[st] - 1 - 1)];
44      graph[[i]] = {Style["Renyi", FontColor -> RGBColor[.2, .2, .2],
             FontFamily -> "Times", FontSize -> 20], Style["q=" <>
            ToString[st[[i]]], FontColor -> color[[i]], FontFamily -> "
            Times", FontSize -> 20]}
45    ];
46   ]
47  , {i, Length[s]}];
48
49  max = Max[Transpose[data[[1]]][[2]]];
50  lp = ListPlot[data, AxesLabel -> {n^2, S[n]}, BaseStyle -> {FontSize
        -> 16}, PlotStyle -> color, ImageSize -> 1000];
51  Do[
52    fpsl[[j]] = Plot[fit[[j]], {x, 0, 2600}, PlotStyle -> color[[j]]]
53  , {j, Length[s]}];
54  Print[Grid[fit, Frame -> True, Alignment -> Left]];
55  rr = LinearModelFit[coeff, {1, 1/y, 1/y^2, 1/y^3, 1/y^4}, y];
56  Print[Normal[rr]];
57  legend = Grid[graph, Alignment -> {{Right, Left}}, Frame -> True];
58  pc = Show[ Plot[rr[y], {y, 0, 4}, PlotRange -> {0, 1}, AxesLabel ->
        {q, \[Alpha][q]}, BaseStyle -> {FontSize -> 16}, ImageSize -> {
        Automatic, 23 Length[st]}], ListPlot[coeff, PlotStyle -> Black
        ]];
59  plot = Show[lp, fpsl, Epilog -> Inset[Grid[{{Rasterize[legend,
        RasterSize -> 1000], pc}}], {700, max - 250}], Frame -> True,
        PlotRangePadding -> 0, FrameLabel -> {n^2, S^{(q)}(n)},
        RotateLabel -> True, ImagePadding -> {{65, 2}, {50, 2}}];
60
61  SetDirectory[pardir <> "\\Graphical␣Results"];
62  Export["Renyi-q_vs_arealaw-c_" <> ToString[fl] <> ".pdf", plot];
63  SetDirectory[pardir];
64  Print[plot];
65  ]
```

These two scripts are import-codes that were nested in scripts D.5 and D.6.

Script D.3 Import data spherical regions

```
dimpsp[NN_, nmax_, dmin_] := Module[{ll, ii, k, l, datsh, datsp},
 SetDirectory[ pardir <> "\\datagen-" <> ToString[NN] <> "-" <>
    ToString[dmin]];
  datsp = ToExpression[
  Import["EE-sp-" <> ToString[NN] <> "-" <> ToString[nmax] <> ".dat"
     , "TSV"]
 ];
 Return[datsp];
 SetDirectory[pardir];
]
```

Script D.4 Import data shell-like regions

```
dimpsh[NN_, nmin_, nmax_, dmin_, rout_] := Module[{ll, ii, k, l,
   datsh, datasp},
 If[rout <= nmax, If[rout > nmin + dmin + 1,
  SetDirectory[ pardir <> "\\datagen-" <> ToString[NN] <> "-" <>
     ToString[dmin] ];
  datsh = ToExpression[
    Import["EE-sh-" <> ToString[NN] <> "-" <> ToString[nmin] <> "-"
       <> ToString[nmax] <> "-" <> ToString[dmin] <>
      "-" <>ToString[rout] <> ".dat", "TSV"]
  ];
  Return[datsh];
  SetDirectory[pardir];
  , Return["wrong input"]], Return["wrong input"]
 ]
]
```

The script below uses the `Do` loop to fill up a predefined array, `data`. This array is then used to build a plot and fit a predicted function against it.

Script D.5 Plot von Neumann entropy of a range of shells

```
shellee[NN_, nmin_, nmax_, dmin_] := Module[{ang, impsh, shee, m,
    data, it, r1, r2, graph, fitq, fitqc},
 ang = 2 NN;
 shee = SparseArray[{}, {nmax, nmax}];
 m = (nmax - dmin - nmin - 2) (nmin + (nmax - dmin - nmin - 1)/2);
 data = SparseArray[{}, {m, 3}];
 it = 1;

 Do[impsh = dimpsh[NN, nmin, nmax, dmin, r2];
  Do[shee[[r1, r2]] = Re[Sum[(2 l + 1) impsh[[l + 1, r1, 4]], {l, 0,
       ang}]];
  shee[[r2, r1]] = shee[[r1, r2]];
  data[[it]] = {r1, r2, shee[[r1, r2]]};
  it++;
  , {r1, 1, r2 - dmin - 1}];
 , {r2, nmin + dmin + 2, nmax - 1}];

 graph = ListPlot3D[Transpose[shee], Mesh -> 5, MeshFunctions -> { #3
     &}, InterpolationOrder -> 1, ColorFunction -> "AvocadoColors",
    AxesLabel -> {n_1 , n_2 , S[n_1, n_2]}, PlotRange -> All,
    ImageSize -> 1500, BaseStyle -> {FontSize -> 22}];
 fitqc = Fit[data, {1, (radius/2)^2 + (radius2 + 1/2)^2}, {radius1,
    radius2}];
 fitq = Fit[data, {(radius1 + 1/2)^2 + (radius2 + 1/2)^2}, {radius1,
    radius2}];

 Print[Grid[{{"Parabolic␣surface␣fit␣:", fitq}, {"Parabolic␣+␣
    constant␣fit␣:", fitqc}}, ItemSize -> All, Frame -> True]];
 Print[Grid[Transpose[data], Frame -> True, ItemSize -> All]];

 SetDirectory[pardir <> "\\Graphical␣Results"];
 Export["shellee-" <> ToString[NN] <> "-" <> ToString[nmin] <> "-" <>
     ToString[nmax] <> "-" <> ToString[dmin] <> ".png", graph];
 SetDirectory[pardir];

 Show[Rasterize[graph]]
 ]
```

Again the shell-based data is imported and thereafter substituted into the definition of the mutual information.

Script D.6 Comparison of analytical and numerical mutual information

```
mutincar[NN_, nmin_, nmax_, dmin_, r1_, r2_] := Module[{l, ang, s1,
    s2, st, mi, micar, dat, impsp, impsh},
 ang = 2 NN;
 impsp = dimpsp[NN, nmax, dmin];
 impsh = dimpsh[NN, nmin, nmax, dmin, r2];
 s1 = Re[Sum[(2 l + 1) impsp[[r1, l + 1]], {l, 0, ang}]];
 s2 = Re[Sum[(2 l + 1) impsp[[r2, l + 1]], {l, 0, ang}]];
 st = Re[Sum[(2 l + 1) impsh[[l + 1, r1, 4]], {l, 0, ang}]];
 mi = (1/r2)^2 (s1 + s2 - st);
 micar = (4 r1^2)/(15 r2^2);
 confmap[NN, r1, r2];
 Print[Grid[{{"ee␣inner␣ball", s1}, {"ee␣outer␣space", s2}, {"ee␣
     shell", s1}, {"num␣mutual␣info", mi}, {"Cardy␣mutual␣info", N[
     micar]}}, Frame -> True, ItemSize -> All]];
 ]
```

Prints some back-of-the-envelope calculations on the conformal mapping in an array.

Script D.7 Additional info for a comparison of mutual information by conformal mapping

```
confmap[NN_, r1_, r2_] := Module[{a, R1, R2, Rout, L, R1p, R2p, Routp
    , R1i, R2i, Routi, dis, disi},
 a = 1/r2;
 R1 = r1/r2;
 R2 = 1;
 Rout = NN/r2;
 L = Sqrt[R1];
 R1p = R1/(R1 - R1^2);
 R2p = R2/(R2^2 - R1);
 Routp = Rout/(Rout^2 - R1);
 R1i = 1;
 R2i = 1/R2;
 Routi = 1/Rout;
 dis = (R2 - R1)/((L + R1) (L + R2));
 disi = 1/Sqrt[R1];
 Print[Grid[{{"uv-cutoff", a, N[a], "␣", "␣", "␣", "␣", "␣", "␣"}, {"
     conformal␣mapping␣point", L, N[L], "mapped␣distance", dis, N[dis
     ], "ideal␣mapped␣dis", disi, N[disi]}, {"inner␣radius", R1, N[R1
     ], "mapped␣first␣radius", R1p, N[R1p], "mapped␣ideal␣1st␣radius"
     , R1i, N[R1i]}, {"outer␣radius", R2, N[R2], "mapped␣second␣
     radius", R2p, N[R2p], "Mapped␣ideal␣2nd␣radius", R2i, N[R2i]}, {
     "outside␣radius", Rout, N[Rout], "mapped␣outside␣radius", Routp,
      N[Routp], "mapped␣ideal␣Rout", Routi, N[Routi]}}, ItemSize -> {
     Automatic, All}, Frame -> {All, True}, Alignment -> Right]];
 ]
```